Externally Bonded Fiber-Reinforced Polymers for Flexural Strengthening of Concrete Beams: Rupture Failure Mode

Naghme Hatami

Avdelningen för Konstruktionsteknik
Lunds Tekniska Högskola
Lunds Universitet, 2004

Kansas State University
Manhattan, Kansas

Rapport TVBK - 5123

Avdelningen för Konstruktionsteknik
Lunds Tekniska Högskola
Box 118
221 00 LUND

Department of Structural Engineering
Lund Institute of Technology
Box 118
S-221 00 LUND
Sweden

Externally Bonded Fiber-Reinforced Polymers for Flexural Strengthening of Concrete Beams: Rupture Failure Mode

Extern fiberarmerings för betong balkar i böjning: Bristning i fiber armering som brottmod.

Naghme Hatami

2004

Abstract

This study provides direct design equations that can be used for FRP reinforced beams with a rupture mode of FRP rupture. An analytical perspective to simplify calculations by developing exact and approximate set of closed form equations is used. This paper is collaboration between the Department of Civil engineering at Kansas State University in Manhattan Kansas and the Department of Structural Engineering at Lund University in Lund, Sweden.

Rapport TVBK-5123
ISSN 0349-4969
ISRN: LUTVDG/TVBK-04/5123+72p

Examensarbete
Handledare: Dr. Hayder A. Rasheed, Sven Thelandersson
Mars 2004

Summary

The subject of external structural strengthening using conventional and innovative materials in buildings and bridges has always been of great interest to researchers and practitioners. One important issue about strengthening with externally bonded steel plates or jackets is corrosion, which can cause significant deterioration to the strengthening system. Innovative materials such as fiber-reinforced polymers (FRP) have been considered as alternative external reinforcement. The idea of using FRP as surface reinforcement is relatively new. Therefore the design of concrete members strengthened with FRP has several different design considerations than that of conventional steel-reinforced concrete members.

Researchers and practicing engineers have recently developed design guidelines for FRP strengthening. However, the current state of the art flexural design procedure suggests an iterative process. The three main flexural failure modes identified for FRP-strengthened beams are brittle concrete crushing (prior to steel yielding), ductile concrete crushing (after steel yielding) and FRP rupture. The FRP rupture failure mode provides the highest section ductility prior to failure, due to the high tensile strength of FRP. However, it also gives a sudden and brittle catastrophic failure due to the sudden release of FRP energy upon rupture. Very little work has been done on the failure mode of FRP rupture to produce direct design equations that can be used by the structural engineer.

This paper provides an analytical perspective to simplify calculations by developing exact and approximate set of closed form equations. It proposes such direct solution to design singly and doubly reinforced, FRP-strengthened rectangular sections. Comparisons with reported experimental data the literature indicate excellent agreement. In order to quantify the accuracy of the approximate equations on a wide range of results, as compared to the exact ones, a parametric study was performed. This study has revealed a yet simpler linear design equation that has an almost perfect statistical correlation.

A similar parametric study is also done for uniaxial FRP wrapped sections. The wrapped sections are interesting because they are reported to limit or control FRP premature separation failure, which may occur with the typical un-wrapped sections, having FRP bonded to the underside (soffit) of beams.

Sammanfattning

Konsten att använda extern strukturell förstärkning med konventionella och innovativa material i byggnader och broar har alltid varit av stort intresse bland forskare och ingenjörer. En stor nackdel med extern armerade stålplattor är korrosion, vilket I sin tur kan leda till en betydande försämring av hållbarheten. Nya material så som fiber-armerad polymer (FRP) har använts som alternativ material för extern armering av betong plattor. Användning av fiber armerad polymer i extern armerade betong plattor är relativt nytt. Det finns därför flera olika hänsynstaganden än för den konventionella stål armeringen.

Nya riktlinjer for design av FRP armering har tagits fram av forskare och ingenjörer, men nuvarande beräkning av böjmoment är en iterativ process.

De tre huvudsakliga böjbrotten som är fastställda för FRP armerade balkar är sprött betong brott (vilket sker innan armeringen uppnår sträckgränstöjning), duktilt betongbrott (töjning i stålet uppnår sträckgränstöjning innan gränsstukningen uppnås i betong) och bristning I FRP. Den sistnämnda brottmoden ger den högsta duktilitet innan brott på grund av FRPs höga draghållfasthet. Däremot sker denna brottmod plötslig och är väldigt sprött på grund av den stora energi mängd som utlöses snabbt vid brott.

Det har skett mycket lite forskning kring denna brottmod för att få fram användbara och enkla ekvationer för att designa dessa balkar.

Syftet med examensarbetet har varit att få fram användbara ekvationer för design av sådana balkar. Detta har gjorts från ett analytiskt perspektiv genom förenkling av beräkningar och därmed givit exakta och approximativa ekvationer för enkelarmerade och dubbelarmerade FRP balkar. Jämförelser med tidigare experimentella data visade sig överensstämma väldigt bra. För att kontrollera noggrannheten för de approximativa ekvationerna, gjordes en stor parametrisk studie, vilket avslöjade en ännu enklare designekvation med en nästan perfekt noggrannhet.

En likadan parametrisk studie gjordes för U-formade FRP plattor. U-formade plattor innebär att fiberplattan förstärker balken även på sidorna förutom på den dragna kanten. Dessa plattor är mycket intressanta eftersom de kan minska risken för tidig platt separation vilken kan ske för balkar med FRP platta fast endast på undersidan av balken.

Acknowledgement

The work presented has been carried out at the Department of Civil Engineering at Kansas State University, Manhattan, Kansas in fall of 2003 and was accepted as a Master Thesis at the Lund Institute of Technology at Lund University.

The project was initiated by Dr. Hayder A. Rasheed who also served as a supervisor during the period of this research. I would like to show my utmost gratitude to Dr. Rasheed for his many ideas and his willingness to share them with me and also for guiding and helping me tremendously during this entire project.

I would also like to thank Prof. Sven Thelandersson for making this collaboration between the Civil Engineering Departments at Lund University and Kansas State University possible.

Also, I would like to thank Mr. Hasan Charkas, who worked with me at the Steam Lab, for providing me with information regarding this work and for helping me along the way.

Finally, I want to thank my fiancé Michael, my parents Dr. Manoucher Hatami and Taraneh Kamali and my sisters, Fati and Neda, for encouraging me and showing me support during this time.

February 2004
Manhattan, Kansas

Naghme Hatami

NOTATIONS

A_s = the area of tensile steel,

A'_s = the area of compressive steel,

A_f = the FRP plate area,

α = f'c multiplier to adjust the height of the equivalent rectangular block to the correct parabolic area,

b = the width of the section,

b_f = the width of the composite plate,

c_n = the neutral axis depth in the section at ultimate,

γ =Neutral axis multiplier yielding the location of the resultant compressive force measured from top of the section,

η = the relationship between the thickness of the bottom flat laminate and the thickness of the vertical FRP reinforcement.

d = the effective depth of the section to steel reinforcement,

d_f = the depth to the centriod of the FRP plate,

h= the height of the section,

h_f =the height of the FRP vertical reinforcement,

d' = the depth of the compressive steel,

E_s = the modulus of elasticity of the steel,

E_f = the FRP plate modulus, ε_o is the strain at the FRP,

E_c = the modulus of elasticity of the concrete,

ε_{fu} = the ultimate strain in the FRP plate,

ε_y = the yielding strain of the steel,

ε_o = the initial deformation in the state of strengthening,

ε'_c = the strain corresponding to f'_c,

ε_{cu}= the compressive strain at crushing of concrete,

ε_{cf}= the concrete strain at FRP rupture,

$\overline{\varepsilon}_{fu}$ = the design ultimate strain in the FRP,

ε_{bi} = Initial tensile strain,

ε_{fv} = FRP strain in the mid-height of the vertical reinforcement,

ε_{fh} = FRP strain in the mid-height of the horizontal reinforcement

ε_s = Strain in steel

ε'_s = Strain in compression steel

f'_c = the compressive strength of the concrete,

f_s = the stress in the steel,

f'_s =the stress in the compression steel,

f_f = the stress in the FRP plate,

f_y = yielding stress of the steel,

f_{fv} = the stress in vertical reinforcement,

f_{fh} = the stress in horizontal reinforcement,

λ = The ratio of the effective FRP tensile force $\rho_f f_{fu}$ to the effective steel tension force $\rho_s f_y$,

$\overline{M}_n$ = the strengthened moment capacity,

M_n = the unstrengthened moment capacity,

M_u = the ultimate design moment,

ρ_f = the ratio of FRP,

ρ_s = the ratio of tension steel,

ρ'_s = the ratio of compression steel,

t_{fv} = the thickness of the vertical reinforcement,

t_{fh} = the thickness of the bottom flat laminate,

y_{fv} =the point of action of the vertical FRP force,

ϕ = the strength reduction factor.

1 Introductory

1.1 Background

Fiber-reinforced polymers (FRP) are non-metallic reinforcements, consisting of high performance fibers such as carbon, glass, aramid and others. The petrochemical industry was the first industry to make these materials available in the early 1940's (ACI.440R-96). Due to the expensive nature of these materials, they were mainly used in the aerospace and defense industry. It wasn't until the 1970's that FRP composite products were first applied to reinforce concrete structures (ACI.440R-96). The interest in FRP materials rose because of its ability to avoid corrosion problems encountered in concrete structures using conventional steel reinforcing bars or pre-stressed tendons. Also, bars and grid reinforcement in concrete that were in harsh environments or required non-magnetic properties would be more suited to be built with FRP. However, the use of FRP as internal reinforcement in main structural members was very limited due to its lack of ductility and higher cost.

By the late 1970's and early 1980's, FRP-composite reinforcing products were demonstrated in Europe and Asia. In 1986, the world's first highway bridge using composite reinforcing tendons was built in Germany. On the other hand, the first research study to use FRP as external jackets for beams and columns was conducted in the U.S. in early 1980's (Fardis and Khalili 1981, 1982). Prof. Meier introduced the first application of FRP as an external strengthening material for existing concrete structures in Switzerland in 1987 (Meier 1987). An extensive amount of experimental research emerged since then throughout the world to qualify this new technology (Bakis et al. 2002). Since the demand for plastic composites grew in the 1990's, the cost of FRP materials decreased and new areas of use were found.

Fiber reinforced polymeric (FRP) composite materials are beginning to find use in construction and infrastructure applications. For the 1990's and beyond, composite fabricators and suppliers are actively developing products for the civil infrastructure, considered to be the largest potential market for FRP composites. Concrete repair and reinforcement, bridge deck repair and new installation, composite-hybrid technology (the marriage of composites with concrete, wood and steel), marine piling and pier upgrade programs are just some of the areas that are currently being explored.

1.2 Objectives

The objective of this study is to develop closed form analytical design equations for rectangular beam sections strengthened with externally bonded FRP that have a failure mode of FRP rupture. The simpler direct equations for the failure mode of ductile concrete crushing were developed earlier (Rasheed and Pervaiz 2003). The study is intended to develop exact and approximate equations that can be directly used in designing members. The first section of this paper focuses on singly reinforced and doubly reinforced concrete rectangular beams. To illustrate the accuracy of the approximate equations on a wide range of results, as compared to the exact ones, an extensive parametric study was performed.

The second part of this study includes developing design equations for sections strengthened with wrapped FRP. It also includes a very extensive parametric study for singly reinforced and doubly reinforced concrete rectangular sections wrapped with FRP.

1.3 Method

This study starts with a presentation of a general overview of the FRP materials to provide an understanding to the different materials in use in the industry and the applications where they are in demand.

The analytical equations developed in this paper will be presented for singly and doubly reinforced sections. Then, they are used to do the necessary verification calculations and to perform the parametric study. These verification designs are taken from various published studies in the literature, where the needed material properties and reported data are also taken. An experimental verification section is also included to demonstrate comparisons with experimental results of previous studies related to this paper. Design examples are selected from existing design guidelines, solved and compared to the results presented in these guidelines.

1.4 Limitations

This work is limited to the development of direct flexural design equations for FRP strengthening considering FRP rupture mode only. It does not cover other failure modes like concrete crushing, shear and plate separation. The study presents original contributions to the literature in this area. Nevertheless, time has been the main factor to limit the scope of work done for this research**.** The parametric study took longer time than expected due to the extensive number of cases considered. This was necessary to examine reliability on the results presented in this paper and has revealed excellent findings that can simplify the design process. Therefore, the priority for the time spent has been dedicated to rectangular beams. It would have been interesting to extend this work to cover T-sections as well.

2 Review of some previous experimental and analytical studies

There is a large volume of studies in the literature addressing FRP strengthening of beams. Most of the research has focused on the premature debonding of FRP sheets. However, this is shown to be controlled by external FRP shear reinforcement (ISIS Canada Design Manual 2001). Accordingly, only publications relevant to the present work are reviewed and summarized below.

Ritchie et al. (1991) tested under-reinforced beams to study the effectiveness of external strengthening using fiber reinforced plastics. The plates bonded to the tension side of the beams were glass, carbon and aramid fibers. Increases in stiffness (over the working load range) from 17 to 99%, and increases in ultimate strength from 40 to 97% were achieved. To predict the strength of the experimental beams tested, a computer technique was used and for prediction of the section response, strain compatibility was used. The experimental failure did not occur in the maximum moment region in many beams, but those that did were within about 5 percent of the predicted load.

An et al. (1991) developed a simplified analytical method to predict stresses and deformations in strengthened beams. Rectangular beams and T-sections were studied for flexural failures. The assumptions made in this analysis are a linear strain distribution through the full depth of the beam, no tensile strength in the concrete, no shear deformations and perfect bond between FRP-plate and the member.

Chajes et al. (1994) tested a series of concrete beams with externally bonded FRP to increase the flexural strength of the beam. The results show that the flexural capacity increased 36-57 % and the flexural stiffness 45-53 %. This paper also makes a comparison between the test results and an analytical model, based on the stress-strain relationships of the concrete, steel and composite fabrics. This comparison indicates the applicability of the method presented in the paper.

Charkas et al. (2003) For calculating deflections of beams, this paper presents an analytical procedure. Comparisons have been made between several experiments to verify the applicability of the presented procedure. The result of the presented procedure, along with those of the ACI traditional equation and modified version of it are compared in a wide range of experimental curves. The result of this comparison shows that the higher the reinforcement stiffness, the higher the modified ACI equations estimate, leading to stiffer deflection predictions. Charkas et al. have also developed simplified calculations to predict the load-deflection response of beams strengthened with FRP plates.

Arduini and Nanni (1997) tested 16 strengthened beams while investigating the effect of surface preparation, beam cross-section, number and location of CFRP (carbon fibers) plies. They predicted the ultimate loads of most of the beams using computer models. The predictions were within 16 percent; however several results were not analyzed. The conclusion is that the performance of pre-cracked beams is not significantly different from the performance of virgin specimens.

Rasheed and Pervaiz (2003) This paper simplifies the calculations used for design of FRP sheets, which would normally give a long, iterative solution. The expressions are given for singly and doubly reinforced sections and also T-sections. Verification against experimental results is performed, and examples are solved to check the capability of the equations. Comparisons with experiments show that effectiveness of the present design equations in accurately estimating the FRP area. Rasheed et al have also shown the suitability of the strengthened reduction factor.

David et al. (1997) studied the behavior of pre-cracked and un-cracked RC beams bonded with varying thickness of CFRP and GFRP plates. The pre-cracked beams were lightly strengthened. The beams, all identical, were tested in 4-point bending and the flexural capacity and failure modes of the beam were investigated. The uncracked beams all failed by the concrete cover separation along the internal reinforcement and the pre-cracked beams failed in FRP rupture. David et al. concluded that FRP changed the failure mode from ductile flexural failure to brittle failure modes.

Triantafillou and Plervis (1992) tested strengthened RC beams and concluded that they can fail in a number of ways. These different failure modes are steel yield-FRP rupture, steel-yield concrete crushing, compressive concrete failure and debonding of the FRP plate. They also tested the beams with the same cross-sectional properties in order to determine whether the FRP area has an effect on the failure mechanism. They concluded that the failure modes became more of a debonding failure as the percentage of the FRP was increased.

Sharif et al (1995) experimentally investigated the repair of initially loaded FRP-reinforced concrete beams. The RC beams are initially loaded to 85 percent of the ultimate flexural capacity and subsequently repaired with FRP plates. The behavior of the repaired beams is then represented by load-deflection curves and the different modes of failure discussed. Sharif et al made the following conclusion based on the experiments. With increasing FRP plate thickness, the shear and normal stresses at the plate curtailment increases and leads to failure by plate separation and concrete rip-off. They also concluded that repaired beams developing their flexural capacities provided enough ductility despite the brittleness of FRP plates.

3 Fiber reinforced polymers

3.1 General use

FRP is attractive for externally bonded applications due to its good tensile strength, low weight and the possibility of bonding to non-flat surfaces. Due to its resistance to corrosion, using FRP as reinforcement solves corrosion problems, which are common in steel reinforced beams and even more serious in beams strengthened by externally bonded steel plates.

Concrete members can benefit from the following features of FRP reinforcement: light weight, high specific strength and modulus, durability, ease of installation, low maintenance cost, corrosion resistance, chemical and environmental resistance, electromagnetic neutrality, and impact resistance

Its main drawbacks are high material cost, relative to steel and sudden brittle failure along the fiber direction.

Another problem, which may occur in strengthened beams, is FRP plate separation. However, earlier research has shown that this premature failure may be avoided by using U-wraps at plate ends and along the beam (Rasheed and Pervaiz 2003, p. 544).

3.2 Composite materials

Composite materials are formed by two or more combinations of materials to form a new material with improved properties (e.g. stiffness, strength or chemical properties). The fibers in the composites provide most of the strength and the stiffness in their direction. The fibers are bound together by the matrix. The matrix also protects the fibers from the environment and carries some of the load and transfers the rest to the fibers by shear. In civil engineering applications, thermosetting resins (thermosets) are almost exclusively used for the matrix. Of the thermosets, epoxy is the one most commonly used.

The major factors affecting the physical performance of the FRP matrix composite are the fiber mechanical properties, fiber orientation, length, shape and composition of the fibers, the mechanical properties of the resin matrix, and the bond between the fibers and the matrix (ACI 440R-96).

The most common fibers used in composites are glass, carbon and organic (aramid) fibers. The mechanical and environmental properties and the cost of fibers are the main factors for choosing which one of the fiber composites to use. A brief review of these materials is presented below.

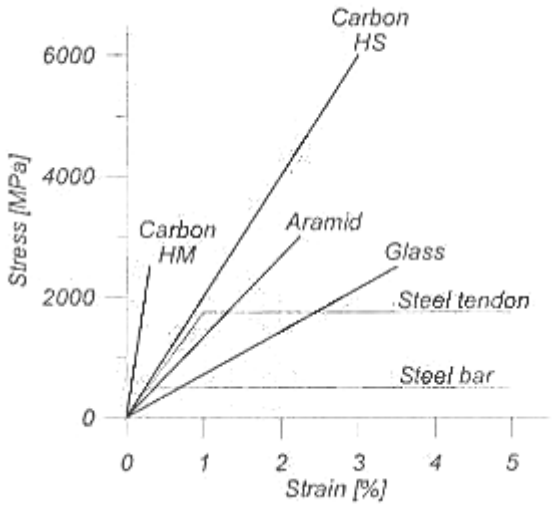

Fig.1. Properties of different fibers and typical reinforcing steel. (ACI.440(1996) and Dejke(2001))

3.2.1 Glass fibers:

Glass has been the foremost type of fiber used for civil engineering purposes because of its *specific* strength properties and economical reasons. The typical properties of glass fibers are harness and corrosion resistance. Glass fibers are elastic until failure and exhibit negligible creep under controlled dry conditions. The modulus of elasticity for glass fibers usually varies between 70-80 GPa. The cured glass-reinforced resin laminate typically have a modulus of 40-45 GPa.

With increased load, the weakest fiber fails first and the other remaining stronger fibers bear the load until they fail in succession.

If exposed to high pH environments, glass can undergo damage over time due to corrosive effects. However, the resin protects the fibers against alkali attack. Extra protection may be gained by using different protective coatings.

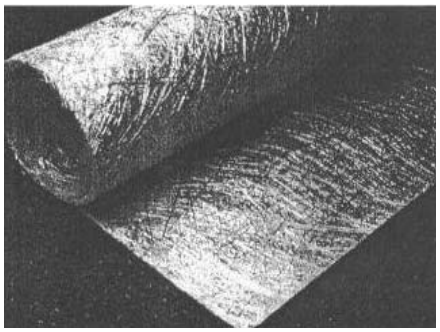

Fig 2. Glass fiber chopped strand mat (Owens-Corning Fiberglass Corporation).

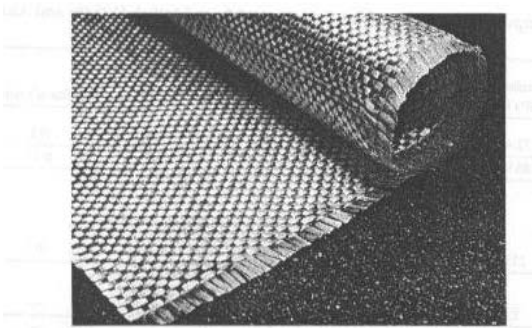

Fig 3. Glass fiber woven roving (Owens-Corning Fiberglass Corporation).

Glass fiber woven roving as shown in Fig 3. is woven fabric of glass. A certain number of parallel, bundled and continuous strands of glass build up these rovings. Since orientation of the fibers can be decided, the properties in different directions can vary.

3.2.2 Carbon fibers:

Carbon fibers have been used mainly in the aerospace market. These fibers are lightweight and have a very good resistance to chemicals and thermal changes.

One advantage of these composites is their wide range of stiffness and strength properties. The raw material and the process used in the manufacturing of these fibers decide its properties. Carbon fibers have a high modulus of elasticity (200-800 GPa) and have excellent fatigue resistance. The fibers also do not show any creep or relaxation.

The major limiting factor for using carbon fibers is the cost. Although being stiffer, lighter and more environmentally stable than glass fibers, the use of carbon fibers is perceived not to be an advantage due to its cost. However, this is the fiber of choice for the majority of external strengthening in civil infrastructure applications.

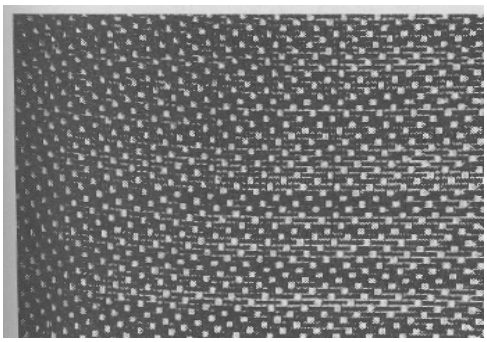

Fig 4. Carbon woven mat

3.2.3 Aramid fibers:

Aramid fibers are a type of organic fibers and the most used one among the organic fibers. Their aromatic ring structure contributes high thermal stability, while the para configuration leads to stiff, rigid molecules that contribute high strength and modulus values comparable to glass**.** (ACI 440R-96)

Aramid fibers have a low density which makes them light weighted, and also during failure they have high energy absorption. However, they have low compressive stain, are sensitive to UV light and change mechanical properties with temperature. The elasticity modulus for aramids is 70-80 GPa.

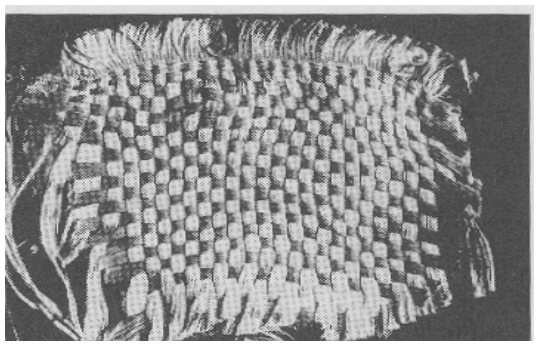

Fig 5. Aramid woven mat

4 Building codes

The design and construction of building are regulated by standard specifications called building codes. These codes usually cover use and occupancy requirements, fire requirements, heating and ventilating requirements, structural design and construction practices. For design specifications of reinforced concrete buildings in the Unites States, *Building Code Requirements for Structural Concrete,* since early 1900's, is used. This code is referred to as the ACI-code and undergoes a revision approximately every four to five years. This paper refers to the ACI code 1999 (ACI-318-99). It also refers to CSA-A23.3-94 (Canadian Standards Association) as the Canadian corresponding document.
In addition to these standard codes, special purpose codes are issued by the same institutions or other supporting organizations. To provide guidance on FRP strengthening, ACI 440.2R-02 and ISIS Canada Design Manuals 2001 were developed.

Design guidelines for FRP external strengthening have recently been developed in North America (ISIS Canada Design Manual 2001, ACI 440.2R-02). The current state of the art flexural design procedure suggests an iterative process. The three main flexural failure modes identified for FRP-strengthened beams are brittle concrete crushing (prior to steel yielding), ductile concrete crushing (after steel yielding) and FRP rupture. The FRP rupture failure mode provides the highest section ductility prior to failure, due to the high tensile strength of FRP. However, it also gives a sudden and brittle catastrophic failure due to the sudden release of the energy stored in the FRP upon rupture. Very little work has been done on the failure mode of FRP rupture to produce direct design equations that can be used by the structural engineer.

ISIS Canada Design Manual 2001 states on page 25 that "In some cases, it may difficult to determine which of the failure modes govern the design. Thus, one may assume a particular failure mode and then verify whether or not this mode does occur. If the initial assumption is incorrect, another mode is assumed and the analysis repeated." The design examples presented, in this manual, are actually analysis problems in which the FRP area is assumed and the section moment capacity is determined. Iterations are needed to adjust the FRP area to provide the required section capacity. Accordingly, the manual provides 102 pages of design charts for singly reinforced sections with varying parameters. In addition to being tedious, the charts give results for specific values of the design parameters, which may require several interpolation steps.

ACI 440.2R-02 follows a similar iterative approach to that depicted by ISIS Canada Design Manual 2001. The design examples also solve for FRP strengthening by assuming an FRP area first then adjusting it while iterating to satisfy the required strengthening capacity.

5 Failure modes

5.1 FRP rupture

In steel-reinforced concrete members, steel yielding before concrete crushing is desirable due to the ductility provided by steel. The other mode of failure of concrete crushing prior to steel yielding may also be allowed. However, the design is taxed by significantly increasing the strength resistance factor (reducing ϕ factor from 0.9 to 0.7).
FRP materials are brittle along the fiber direction with a linear stress-strain curve until failure, and will therefore give a sudden and brittle failure mode.
The failure mode upon which this study is based, is FRP rupture. Therefore the strain in the extreme concrete fiber in compression at FRP-failure will be unknown, and will be written as ε_{cf} in this paper.

5.2 Concrete Crushing

Concrete crushing occurs when the strain in concrete reaches its ultimate value of 0.003.
For under-reinforced sections the steel will yield before the concrete crushing. This results in a ductile failure characterized by large amounts of energy absorbed through plastic straining in the reinforced steel. Large deflection will take place forcing the strain in the concrete to reach its ultimate value, so ultimately the under-reinforced beam will fail in flexural compression.

Over-reinforced concrete members will fail in a brittle failure mode, where the concrete will fail before the yielding of the steel. The crack pattern by the reinforcement will be small due to the fact that no plasticity occurs in the steel. However the cracking area in the compression area is wide.

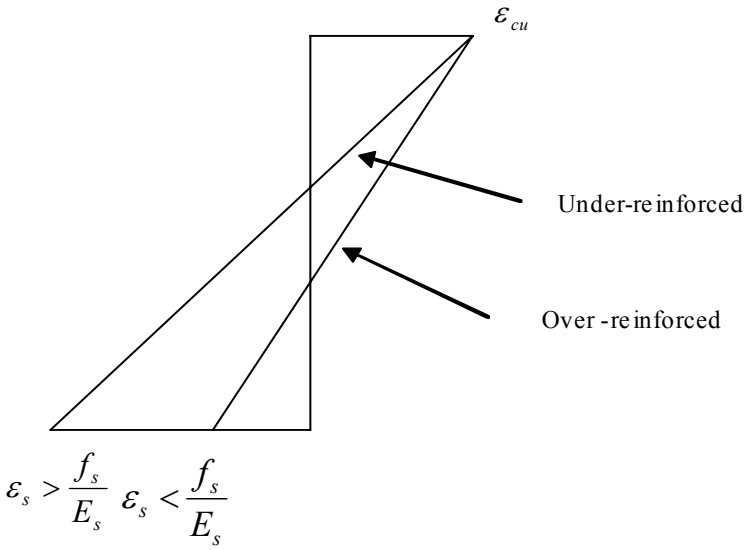

Fig 6. Strain distribution for over-reinforced and under-reinforced sections, where ε_s =strain in steel

5.3 Minimum FRP reinforcement ratio

5.3.1 Singly reinforced sections

Our equations are based on the FRP rupture failure mode. To ensure that this mode of failure controls the design, the FRP ratio is kept lower than the minimum balanced ratio, which would cause simultaneous concrete crushing and FRP rupture. The equation for this ratio is developed by Rasheed and Pervaiz (2003), as follows:
The strain compatibility at the simultaneous concrete crushing and FRP rupture will give
the following expression:

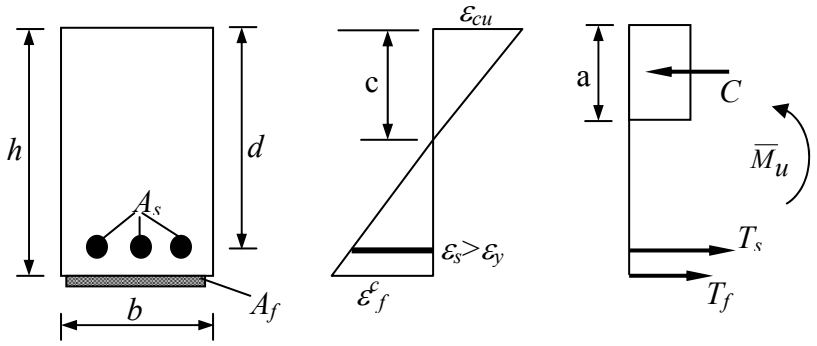

Fig 7. Singly reinforced cross section with strain distribution and force profile at balanced failure

$$\frac{\varepsilon_{cu}}{c_b^{\min}} = \frac{\varepsilon_{cu} + \bar{\varepsilon}_{fu}}{h} \tag{1}$$

where $\bar{\varepsilon}_{fu} = \varepsilon_{fu} + \varepsilon_{bi}$, ε_{fu} is the design ultimate strain in the FRP, ε_{bi} is the initial tensile strain at the bottom of the section due to pre-existing loads during strengthening, ε_{cu} = 0.003 at concrete crushing. Accordingly, the following expression is obtained for the balanced location of neutral axis ($c_b^{\min}$):

$$c_b^{\min} = \frac{0.003h}{0.003 + \bar{\varepsilon}_{fu}} = \frac{a_b^{\min}}{\beta_1} \tag{2}$$

The force equilibrium for the section is

$$0.85 f'_c b a_b^{\min} = A_s f_y + A_f^{b\min} f_{fu} \tag{3}$$

This will give the minimum ratio of FRP

$$\rho_f^{b\min} = 0.85 \frac{f'_c}{f_{fu}} \left(\frac{a_b^{\min}}{d}\right) - \rho_s \frac{f_y}{f_{fu}} \tag{4}$$

where $\rho_f^{b\min} = \frac{A_f^{b\min}}{bd}$ and $\rho_s = \frac{A_s}{bd}$

5.3.2 Doubly reinforced sections

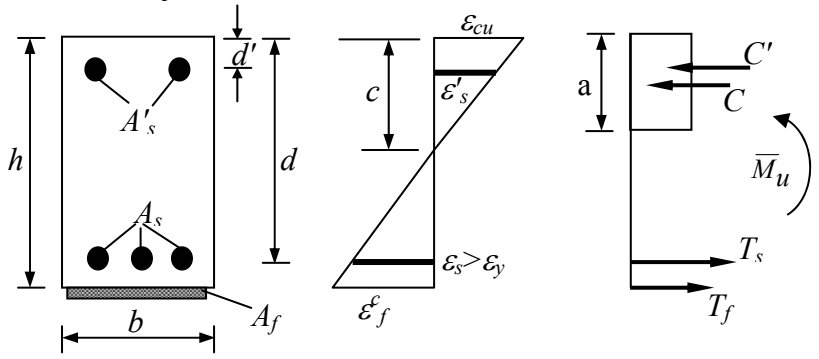

Fig 8. Doubly reinforced cross section with strain distribution and force profile at balanced failure

The strain compatibility is used to define the compressive steel strain, Fig 8.

$$\frac{\varepsilon_{cu}}{c_n} = \frac{\varepsilon_{cu} - \varepsilon'_s}{d'} \qquad (5)$$

At concrete crushing the value of $\varepsilon_{cu} = 0.003$ is assumed to apply.

$$\Rightarrow \varepsilon'_s = 0.003(1 - \frac{d'}{c_n}) = 0.003(1 - \frac{\beta_1 d'}{a}) \qquad (6)$$

The expression for a minimum FRP ratio for doubly reinforced sections $\rho_f^{\sim b\min}$ was then formulated to be:

$$\rho_f^{\sim b\min} = \rho_f^{b\min} + \rho'_s \frac{f'^{b\min}_s}{f_{fu}} \qquad (7)$$

where

$$f'^{b\min}_s = fy, \qquad \text{if } \frac{d'}{h} \le \frac{600 - f_y}{600 + 200000(\varepsilon_{fu} + \varepsilon_0)}$$

$$f'^{b\min}_s = 600 - \frac{d'}{h}(600 + 200000(\varepsilon_{fu} + \varepsilon_0)), \qquad \text{otherwise}$$

Where $f'^{b\min}_s$ is the stress of the compression steel and ε_0 is the initial deformation in the state of strengthening.

6. Behavior of constituent materials

6.1 Stress-strain relationship of steel

Reinforcing steel is assumed to have an elastic-perfectly plastic stress-strain curve, Fig. 9.

$$\varepsilon_y = f_y E_s \quad (8)$$

where ε_y = yielding strain, f_y = yielding strength and E_s = modulus of elasticity of steel. This model assumes that plastic flow occurs as the stress reaches the yield stress f_y .

It is an accurate representation for yield strength values up to 414 MPa (60 ksi). High- strength steel exhibit nonlinear yielding region. However, this can still be expressed in terms of effective yield strength.

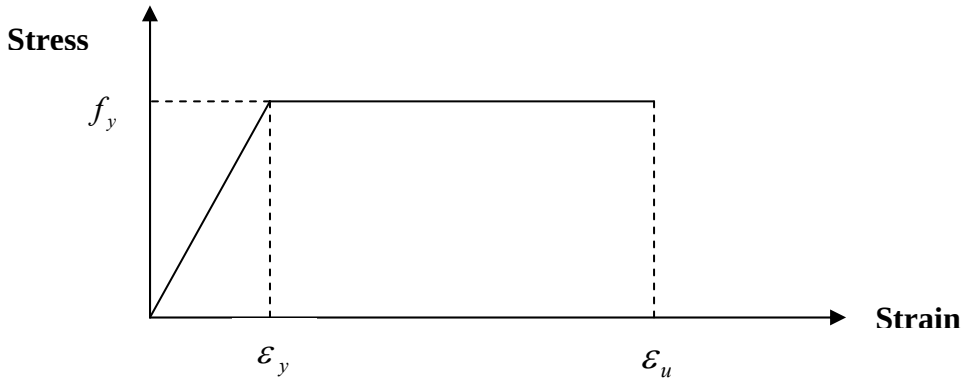

Fig 9. Steel behavior in tension and compression

6.2 Stress-strain relationship of concrete

Since the dominant failure mode is FRP rupture, concrete extreme fiber in compression may not reach crushing ($\varepsilon_{cf} < 0.003$). Accordingly, the typical parameters of Whitney's stress block, used for steel-reinforced members, cannot be directly applied. Consequently, the idealized stress block is re-formulated to take the actual stress-strain distribution into account. The following description and formulation use the analytical concrete stress-strain relationship proposed by Hognestad et al. (1955), Fig. 10, expressed as:

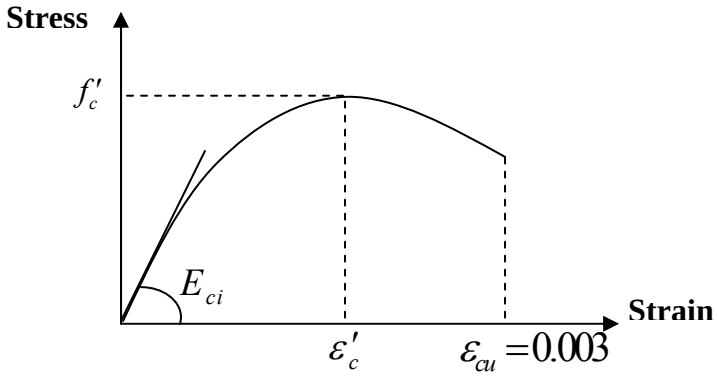

Fig 10. Stress-strain behavior of concrete in compression

$$\sigma_c = f_c' \left[2\frac{\varepsilon_c}{\varepsilon_c'} - \left(\frac{\varepsilon_c}{\varepsilon_c'} \right)^2 \right] \qquad (9)$$

where *f'c* is the compressive strength of concrete and ε'c is the strain corresponding to *f'c*. Based on Hogenstad's parabolic stress-strain curve, a factor, α ,is used to convert the non-linear stress-strain relationship into an equivalent rectangular distribution for the same strain range.

$$\alpha = \frac{\int_0^{\varepsilon_{cf}} \sigma_c d\varepsilon_c}{f_c' \varepsilon_{cf}} = \frac{\varepsilon_{cf}}{\varepsilon_c'} - \frac{\varepsilon^2{}_{cf}}{3\varepsilon'^2} \qquad (10)$$

where ε_{cf} is the concrete extreme fiber compression strain at FRP rupture. This strain (ε_{cf}) is expressed in terms of the FRP ultimate rupture strain using the following strain compatibility equation, Fig 11:

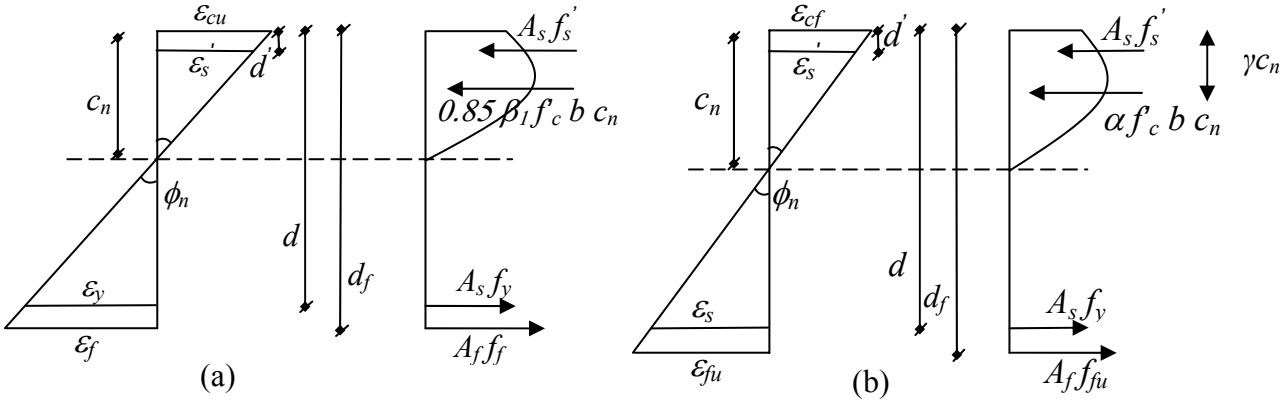

Fig 11. Section strain-compatibility relationships (a) at concrete crushing and (b) at FRP rupture

$$\frac{\varepsilon_{cf}}{c_n} = \frac{\overline{\varepsilon}_{fu}}{h - c_n} \Rightarrow \varepsilon_{cf} = \frac{\overline{\varepsilon}_{fu} c_n}{h - c_n} \qquad (11)$$

where $\overline{\varepsilon}_{fu} = \varepsilon_{fu} + \varepsilon_{bi}$, ε_{fu} is the design ultimate strain in the FRP, ε_{bi} is the initial tensile strain at the bottom of the section due to pre-existing loads during strengthening. Substituting equation (11) into equation (10), the parameter α is written in terms of the depth of neutral axis (c_n):

$$\alpha = \frac{\overline{\varepsilon}_{fu} c_n}{(h - c_n)\varepsilon_c'} - \frac{(\overline{\varepsilon}_{fu} c_n)^2}{(h - c_n)^2 3\varepsilon_c'^2} \qquad (12)$$

The point of action of the compressive force of concrete *C*, measured from the extreme compression fiber of concrete, is written as a fraction of the neutral axis depth (γc_n). The expression for γ is derived as follows, (Park and Paulay 1975):

$$\gamma = 1 - \frac{\int_0^{\varepsilon_{cf}} \varepsilon_c \sigma_c d\varepsilon_c}{\varepsilon_{cf} \int_0^{\varepsilon_{cf}} f_c d\varepsilon_{cf}} = \frac{\frac{1}{3} - \frac{\varepsilon_{cf}}{12\varepsilon'_c}}{1 - \frac{\varepsilon_{cf}}{3\varepsilon'_c}} \qquad (13)$$

Substituting equation (11) into equation (13), the parameter γ is written in terms of the depth of neutral axis (c_n):

$$\gamma = \frac{4\varepsilon'_c h - c_n(4\varepsilon_c + \varepsilon_{fu})}{12\varepsilon'_c h - c_n(12\varepsilon'_c + 4\varepsilon_{fu})} \qquad (14)$$

6.3 Stress-strain relationship of the FRP composite

The FRP, along the fiber direction, has a linear stress-strain curve until brittle failure. Therefore, it is considered to behave linearly elastic up to such rupture failure, Fig. 12.

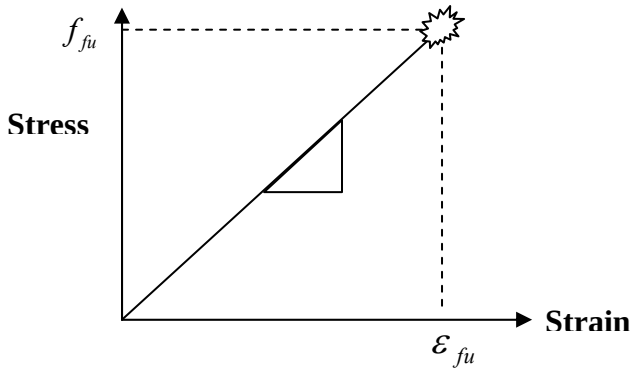

Fig 12 FRP stress-strain curve in tension along fiber direction.

7 Design equations for FRP rupture in flat laminates

7.1 Exact solution

7.1.1 Singly reinforced rectangular sections:

Reinforced concrete sections are completely solved if strain compatibility and force equilibrium equations are simultaneously applied by imposing constitutive relationships, such as those presented in section 5. The force equilibrium equation, at FRP rupture condition, for the singly reinforced section is:

$$\sum F_x = 0 \Rightarrow \quad \alpha f_c' b c_n - A_s f_y - A_f f_{fu} = 0 \qquad (15)$$

The moment equilibrium equation about the centroid of FRP plate for this section is:

$$M_u = \phi M_n = \phi \alpha f_c' b c_n (h - \gamma c_n) - \phi A_s f_y (h - d) \qquad (16)$$

where M_u is the ultimate design moment of the strengthened section, ϕ=0.9 is the strength reduction factor as defined by ACI 318-99 and ACI 440.2R-02, M_n is the nominal moment capacity of the strengthened section, A_s is the tension steel reinforcement in the section and d is the effective depth from the top of the section to the centroid of A_s. The concrete strain ε_{cf} is related to the FRP rupture strain using strain compatibility, as follows, Fig. 11b:

$$\frac{\varepsilon_{cf}}{c_n} = \frac{\bar{\varepsilon}_{fu}}{h - c_n} \Rightarrow \varepsilon_{cf} = \frac{\bar{\varepsilon}_{fu} c_n}{h - c_n} \qquad (17)$$

By re-arranging the moment equilibrium expression, equation (16) above:

$$\frac{M_u}{\phi f_c' b h^2} = \frac{M_n}{f_c' b h^2} = \frac{\alpha c_n (h - \gamma c_n)}{h^2} - \rho_s \frac{f_y}{f'_c} \frac{d}{h} \left(1 - \frac{d}{h}\right) \qquad (18)$$

where $\rho_s = \frac{A_s}{bd}$. Grouping the second term on the right hand side with the left hand side term as Q_u, equation (18) above becomes:

$$Q_u - \frac{\alpha c_n (h - \gamma c_n)}{h^2} = 0 \qquad (19)$$

where $Q_u = \frac{M_n}{f_c' b h^2} + \rho_s \frac{f_y}{f_c'} \frac{d}{h} \left(1 - \frac{d}{h}\right)$

Substituting the α and γ expressions above, equations (12) and (13), into equation (19), and manipulating the tedious algebraic operation, the following exact 5th degree polynomial, in terms of the depth of the neutral axis (c_n), is obtained:

$$A\frac{c_n}{h} + B(\frac{c_n}{h})^2 + D(\frac{c_n}{h})^3 + E(\frac{c_n}{h})^4 + F(\frac{c_n}{h})^5 - 12Q_u\varepsilon'_c = 0 \qquad (20)$$

where

$$A = Q_u(4\overline{\varepsilon}_{fu} + 36\varepsilon'_c)$$

$$B = \overline{\varepsilon}_{fu}(12 - 8Q_u) - 36Q_u\varepsilon'_c$$

$$D = -28\overline{\varepsilon}_{fu} - \frac{(\overline{\varepsilon}_{fu})^2}{\varepsilon'_c} + Q_u(12\varepsilon'_c + 4\overline{\varepsilon}_{fu})$$

$$E = \overline{\varepsilon}_{fu}(16 + \frac{23\overline{\varepsilon}_{fu}}{3\varepsilon'_c} + \frac{4(\overline{\varepsilon}_{fu})^2}{3(\varepsilon'_c)^2})$$

$$F = -\frac{\overline{\varepsilon}_{fu}}{\varepsilon'_c}(4\varepsilon'_c + \overline{\varepsilon}_{fu})(1 + \frac{\overline{\varepsilon}_{fu}}{3\varepsilon'_c})$$

Solving equation (20) above for it 5 roots, the lowest positive root yields the value of c_n. By using the force equilibrium, equation (15), the amount of FRP reinforcement needed, is consequently determined. The ratio for FRP reinforcement is:

$$\rho_f = \alpha\frac{f'_c}{f_{fu}}(\frac{c_n}{h}) - \rho_s\frac{f_y}{f_{fu}} \qquad (21)$$

where $\rho_f = \frac{A_f}{bd}$

7.1.2 Doubly reinforced section

Doubly reinforced sections have both tension and compression reinforcement. The main complication in design occurs when the compression steel is located close enough to the neutral axis such that it does not yield at failure. Both cases, where the compression reinforcement yields and does not yield, are presented in this paper.

The force equilibrium equation, at FRP rupture condition**,** for a doubly reinforced section is:

$$\sum F_x = 0 \Rightarrow \alpha f'_c\, b c_n - A_s f_y - A_f f_{fu} + A'_s\, f'_s = 0 \qquad (22)$$

As for the singly reinforced section, the moment equilibrium is taken about the centroid of the FRP plate:

$$Mu = \phi Mn = \alpha f'_c\, b c_n (h - \gamma c_n) - A_s f_y (h - d) + A'_s\, f'_s\, (h - d') \qquad (23)$$

where A'_s is the compression steel reinforcement in the section and d' is the top cover depth to the centroid of A'_s, f'_s is the stress in compression steel related to the FRP rupture strain using strain compatibility, as follows, Fig. 11b:

$$\varepsilon'_s = \varepsilon_{cf}\,(1 - \frac{d'}{c_n}) \qquad (24)$$

Accordingly, a verification calculation must be done to check whether the compression steel will yield or not. Since it is typically assumed that the compression steel will always yield first hand, f_y is substituted, in the trial attempt, for the stress in the compression reinforcement (f'_s).

7.1.2.1 Yielding of compression reinforcement

Invoking equation (23) and re-arranging its terms:

$$\frac{Mu}{\phi f'_c b h^2} = \frac{Mn}{f'_c b h^2} = \frac{\alpha c_n (h - \gamma c_n)}{h^2} - \rho_s \frac{f_y}{f'_c}\frac{d}{h^2}(1 - \frac{d}{h}) + \rho'_s \frac{f_y}{f'_c}\frac{d}{h}(1 - \frac{d'}{h}) \qquad (25)$$

where $\rho'_s = \frac{A'_s}{bd}$. Grouping the Q_u term, defined earlier, with the third term on the right hand side as Q'_u, equation (25) above becomes:

$$Q'_u - \frac{\alpha c_n (h - \gamma c_n)}{h^2} = 0 \qquad (26)$$

where $Q'_u = Q_u - \rho'_s \frac{f_y}{f'_c}\frac{d}{df^2}(1 - \frac{d'}{df})$.

Substituting equations (12) and (13) into (26) and manipulating the tedious algebraic steps, equation (27) will give the 5th degree polynomial needed to exactly solve for the neutral axis depth (c_n):

$$A'\frac{c_n}{h} + B'(\frac{c_n}{h})^2 + D'(\frac{c_n}{h})^3 + E'(\frac{c_n}{h})^4 + F'(\frac{c_n}{h})^5 - 12Qu'\varepsilon'_c = 0 \qquad (27)$$

where

$$A' = Q'_u\,(4\bar{\varepsilon}_{fu} + 36\varepsilon'_c)$$

$$B' = \bar{\varepsilon}_{fu}(12 - 8Q'_u) - 36\varepsilon'_c\,Q'_u$$

$$D' = -28\bar{\varepsilon}_{fu} - \frac{\bar{\varepsilon}_{fu}^{\,2}}{\varepsilon'_c} + Q_u'(12\varepsilon'_c + 4\bar{\varepsilon}_{fu})$$

$$E' = E$$

$$F' = F$$

7.1.2.2 No yielding of the compression reinforcement

When $\varepsilon'_s < \varepsilon_y$, the compression steel will not yield at FRP rupture. Therefore, the stress in the compressive reinforcement is calculated as $f'_s = \varepsilon'_s\,E'_s$. The moment equation will slightly change as follows:

$$\frac{M_u}{\phi f'_c bh^2} = \frac{M_n}{f'_c bh^2} = \frac{\alpha c_n(h-\gamma c_n)}{h^2} - \rho_s\frac{f_y}{f'_c}\frac{d}{h}(1-\frac{d}{h}) + \rho'_s\frac{\varepsilon'_s E'_s}{f'_c}\frac{d}{h}(1-\frac{d'}{h}) \qquad (28)$$

Re-writing equation (28) in terms of Q_u:

$$Q_u - \frac{\alpha c_n(h-\gamma c_n)}{h^2} - \rho' s\frac{\varepsilon'_s E'_s}{f'c}\frac{d}{h}(1-\frac{d'}{h}) = 0 \qquad (29)$$

Substituting equations (12) and (13) and (24) into (29) and manipulating the tedious algebraic steps, equation (30) will give the 5th degree polynomial needed to exactly solve for the neutral axis depth (c_n):

$$A'\frac{c_n}{h} + B'(\frac{c_n}{h})^2 + D'(\frac{c_n}{h})^3 + E'(\frac{c_n}{h})^4 + F'(\frac{c_n}{h})^5 - Q_u G = 0 \qquad (30)$$

where

$$A' = A + G(h + d')$$

$$B' = B - G$$

$$D' = D$$

$$E' = E$$

$$F' = F$$

$$G = \rho'_s\frac{E_s\varepsilon'_s}{f'_c}\frac{d}{h}(1-\frac{d'}{h})$$

7.1.2.3 Determining FRP reinforcement ratio

The ratio of FRP reinforcement is simply calculated for the doubly reinforced section by using the force equilibrium, equation (23), after obtaining c_n from equation (27) or (30).

$$\rho_f = \alpha \frac{f'_c}{f_{fu}}\left(\frac{c_n}{h}\right) - \rho_s \frac{f_y}{f_{fu}} + \rho'_s \frac{f_y}{f_{fu}} \qquad (31)$$

7.2 Approximate solution

7.2.1 Singly reinforced section

The 5th degree polynomial equations above can be simplified using rational approximate expressions for the α and γ factors in equations (12) and (13). The concrete strain corresponding to f'_c (ε'_c) is known to be closely approximated by 0.002 for normal and moderately high strength concrete. Substituting the constant value of ε'_c into equations (13) and (14), the relationship between α and γ in terms of ε_{cf} can be expressed and plotted as shown below:

$$\alpha = 500\varepsilon_{cf} - 83333\varepsilon_{cf}^{\,2} \qquad (32)$$

$$\gamma = \frac{0.33 - 41.67\varepsilon_{cf}}{1 - 166.67\varepsilon_{cf}} \qquad (33)$$

The γ expression in equation (33) will be significantly simplified if a linear γ regression function of ε_{cf} is generated with an excellent coefficient of correlation (R^2=0.9677), see Fig. 13:

$$\gamma = 27.768\varepsilon_{cf} + 0.3239 \qquad (34)$$

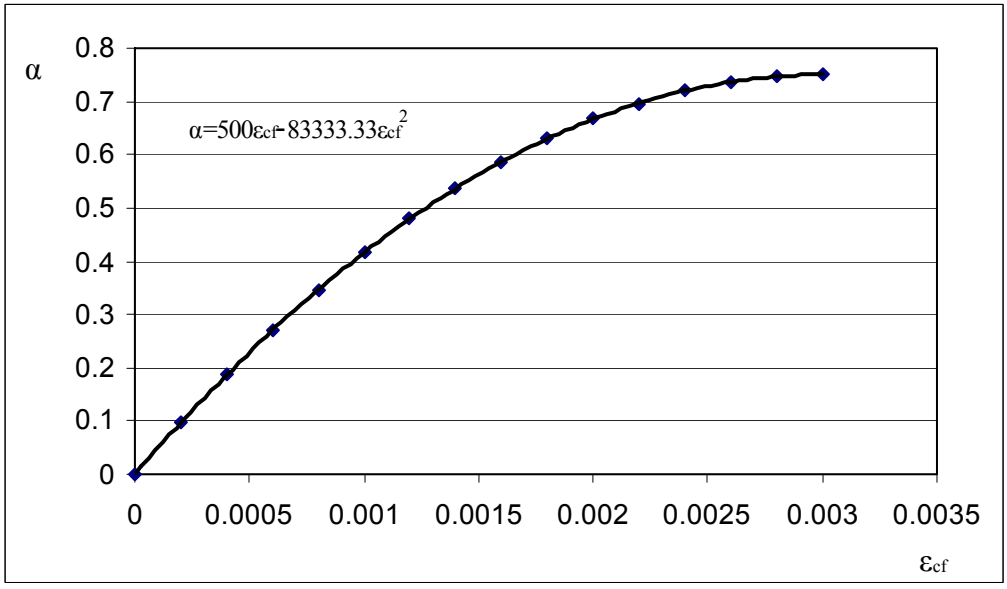

Fig. 13 Quadratic regression plot of α vs. ε_{cf} relationship.

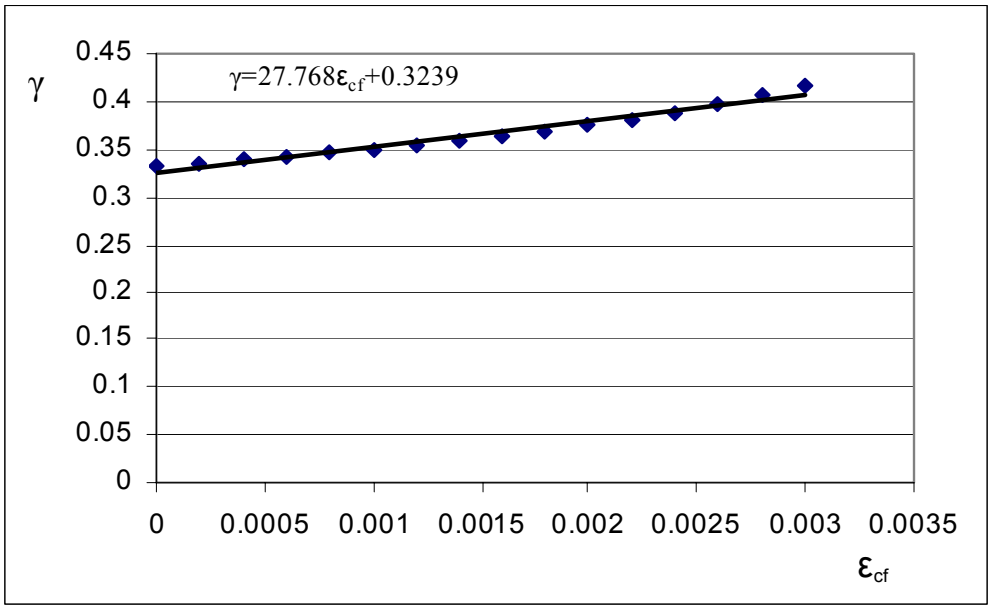

Fig. 14. Linear regression plot of γ vs. ε_{cf} relationship.

Equation (32) still presents no simplification for the α expression. Observing the discrete α points on Fig. 13, one may notice that the parabolic curve may be approximated by two straight lines with a breaking point where they change slope at around ε_{cf} = 0.0015. Fitting the two ranges of ε_{cf} by two least square lines, the following approximate equations are generated for α with excellent coefficients of correlation (R^2=0.9931, 0.9305), Fig. 15:

$$\alpha = 366.67\varepsilon_{cf} + 0.0417 \qquad 0 \le \varepsilon_{cf} < 0.0015 \qquad (35a)$$

$$\alpha = 125\varepsilon_{cf} + 0.4042 \qquad 0.0015 \le \varepsilon_{cf} \le 0.003 \qquad (35b)$$

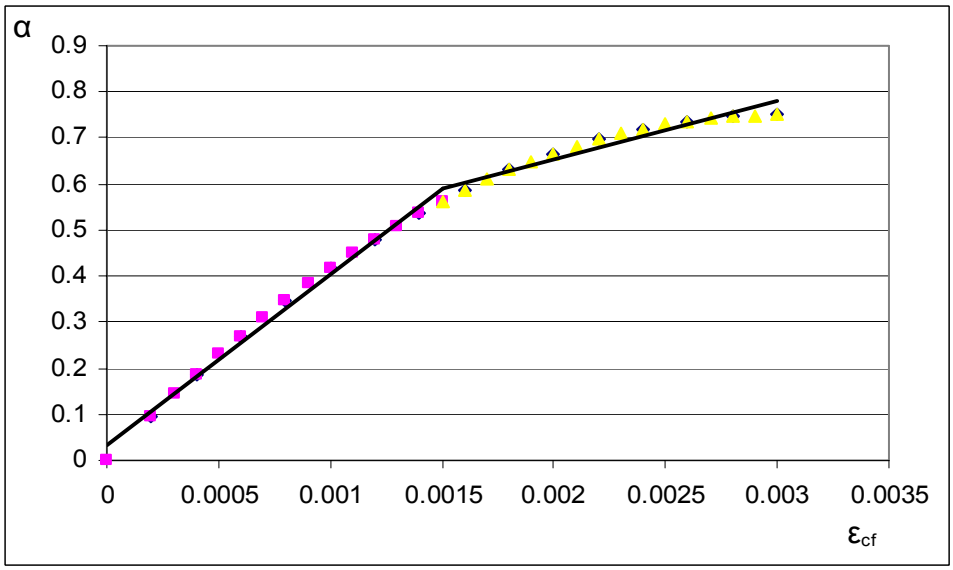

Fig. 15 Linear regression relationships of α vs. εcf.

In addition, the values of α in Fig. 15 are seen to have a slight variation along the entire range of ε_{cf}. Accordingly, equation (34) may be further simplified by considering two constant values of γ for the two ranges of strain identified above in the case of α. These constant values are selected to be the average of the two end values of each strain range:

$$\gamma = \frac{\gamma_0 + \gamma_{0.0015}}{2} = 0.3447 \qquad 0 \le \varepsilon_{cf} \le 0.0015 \qquad (36a)$$

$$\gamma = \frac{\gamma_{0.0015} + \gamma_{0.003}}{2} = 0.3911 \qquad 0.0015 \le \varepsilon_{cf} \le 0.003 \qquad (36b)$$

By substituting equations (35a and b) and (36a and b) into the moment equilibrium, equation (19), an 3rd degree approximate polynomial equation will be developed:

$$A_3 \frac{c_n}{h} + B_3 (\frac{c_n}{h})^2 + D_3 (\frac{c_n}{h})^3 - Q_u = 0 \qquad (37)$$

where

$For\ \varepsilon_{cf} \le 0.0015:$	$For\ 0.0015 < \varepsilon_{cf} \le 0.003:$
$A_3 = 0.0417 + Q_u$	$A_3 = 0.4042 + Q_u$
$B_3 = 366.67\varepsilon_{fu} - 0.056$	$B_3 = 125\varepsilon_{fu} - 0.246$
$D_3 = -126.4\varepsilon_{fu} + 0.014375$	$D_3 = -48.866\varepsilon_{fu} + 0.1581$

The approximate equations are easier to apply than the exact ones and can be directly solved for c_n using a scientific calculator. Once c_n is determined, the ratio of FRP reinforcement is directly obtained from equation (21).

7.2.2 Doubly reinforced section

As for singly reinforced sections, the same approximations are done for the doubly reinforced sections. The approximate equations are expressed in terms of the yielding status of compression reinforcement, as presented earlier:

7.2.2.1 Yielding of compression steel

The cubic equation of c_n changes to:

$$A_3 \frac{c_n}{h} + B_3 (\frac{c_n}{h})^2 + D_3 (\frac{c_n}{h})^3 - Q'_u = 0 \qquad (38)$$

where A_3, B_3, D_3 are defined above and Q'_u is defined earlier in the exact solution, equation (26).

7.2.2.2 No yielding of compression steel

The cubic equation in c_n becomes:

$$A_3' \frac{c_n}{h} + B_3' (\frac{c_n}{h})^2 + D_3' (\frac{c_n}{h})^3 - Q_u h - Gd' = 0 \qquad (39)$$

where

$A_3' = A_3 + G$

$B_3' = B_3$

$D_3' = D_3$

G is defined under equation (30).

The approximate equations (38) or (39) are easy to solve for c_n, as the smallest positive root, using a scientific calculator. The FRP reinforcement ratio for doubly reinforced sections is directly calculated using the equation (31).

8. Design equations for FRP rupture mode in wrapped laminates

More efficient flexural FRP strengthening may be achieved when the uniaxial laminates are wrapped around the bottom of the beam section up the sides, especially if it is terminated above the steel reinforcement level. This provides external confinement to the concrete cover, shifts the weak plane of horizontal shear upwards and allows for lower interface shear stresses by increasing the bond surface per FRP reinforcement area. However, this practical improvement presents a further complication to the already involved design equations. The contribution of side FRP enters into the moment equilibrium equation causing the c_n polynomial to assume yet a higher degree.

8.1 Singly reinforced rectangular sections

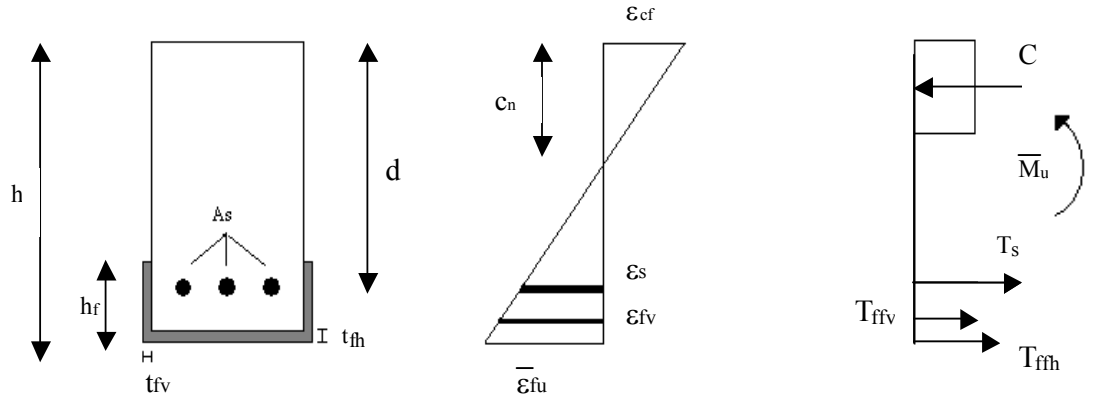

Fig 16. Singly reinforced section with wrapped laminate.

Invoking the strain compatibility equation for the concrete extreme compression fiber and the FRP side reinforcement:

$$\varepsilon_{cf} = \frac{\varepsilon_{fu} c_n}{h - c_n} \tag{40a}$$

$$\varepsilon_{fv} = \frac{\varepsilon_{fu}}{h - c_n}(h - c_n - \frac{h_f}{2}) \tag{40b}$$

where ε_{fv} = FRP strain in the mid-height of the vertical reinforcement and h_f = the height of the FRP vertical reinforcement

The force equilibrium for the a singly reinforced section with wrapped FRP is:

$$\sum F_x = 0 \Rightarrow \quad \alpha f_c' b c_n - A_s f_y - A_{fv} f_{fv} - A_{fh} f_{fh} = 0 \tag{41}$$

where

$$\begin{aligned} f_{fv} &= E_f \varepsilon_{fv}, \quad A_{fv} = 2 h_f t_{fv} \\ f_{fh} &= E_f \varepsilon_{fu}, \quad A_{fh} = b t_{fh} \end{aligned} \tag{42}$$

t_{fv} = thickness of the vertical FRP reinforcement, t_{fh} = thickness of the bottom flat laminate and ε_{fu} = the design rupture strain of FRP. To consolidate the number of unknowns, the thickness of the flat FRP sheets is expressed in terms of the thickness of vertical sheets.

$$t_{fh} = \eta t_{fv} \tag{43}$$

Substituting equations (40), (42) and (43) into (41), the force equilibrium equation becomes:

$$\alpha f_c' b c_n = A_s f_y + b \eta t_{fv} E_f \varepsilon_{fu} + 2 h_f t_{fv} E_f \frac{\varepsilon_{fu}}{h - c_n}(h - c_n - \frac{h_f}{2}) \tag{44}$$

Solving for t_{fv}, one obtains:

$$t_{fv} = \frac{(\alpha f_c' b c_n - A_s f_y)(h - c_n)}{f_{fu}[\eta b (h - c_n) + 2 h_f (h - c_n - \frac{h_f}{2})]} \tag{45}$$

The moment equilibrium equation about the level of horizontal FRP plate is:

$$M_u = \phi M_n = \phi \alpha f_c' b c_n (h - \gamma c_n) - \phi A_s f_y (h - d) - \phi A_{fv} f_{fv} y_{fv} \tag{46}$$

where y_{fv} = the point of action of the vertical FRP force:

$$y_{fv} = \frac{h_f}{3}(\frac{2\varepsilon_{fv} + \varepsilon_{fu}}{\varepsilon_{fv} + \varepsilon_{fu}}) \tag{47}$$

The variable y_{fv} is in between $h_f/2$ and $h_f/3$, expected to be closer to $hf/2$. To simplify the moment equation, $h_f/2$ is conservatively substituted for y_{fv}. Substituting equations (40b) and (45) into (46):

$$\frac{M_u}{\phi f_c' b h^2} = \frac{M_n}{f_c' b h^2} = \frac{\alpha c_n (h - \gamma c_n)}{h^2} - \rho_s \frac{f_y}{f_c'} \frac{d}{h} (1 - \frac{d}{h})$$
$$- (\frac{h_f}{h})^2 (\alpha c_n - \rho_s \frac{f_y}{f_c'} d) \frac{(h - c_n - \frac{h_f}{2})}{[\eta b (h - c_n) + 2 h_f (h - c_n - \frac{h_f}{2})]}$$

$$\Rightarrow \left[\frac{\alpha c_n (h - \gamma c_n)}{h^2} - Q_u \right] \left[\eta b (h - c_n) + 2 h_f (h - c_n - \frac{h_f}{2}) \right]$$
$$- (\frac{h_f}{h})^2 (\alpha c_n - \rho_s \frac{f_y}{f_c'} d)(h - c_n - \frac{h_f}{2}) = 0 \qquad (48)$$

Further simplification of equation (48) yields a 6th degree polynomial in c_n when the exact expressions of α and γ are used and a 4th degree polynomial in c_n when their approximate equations are substituted. However, it is evident that the resulting expression will be very lengthy and it is, thus, avoided. Instead, equation (44) is repeatedly solved for c_n by assuming a large number of values for the FRP area and finding the corresponding M_n exactly from equations (46) and (47), in an analysis mode. Then, the results are correlated in an extensive parametric study to develop simple expressions that can be used in both design and analysis calculations.

8.2 Doubly reinforced section

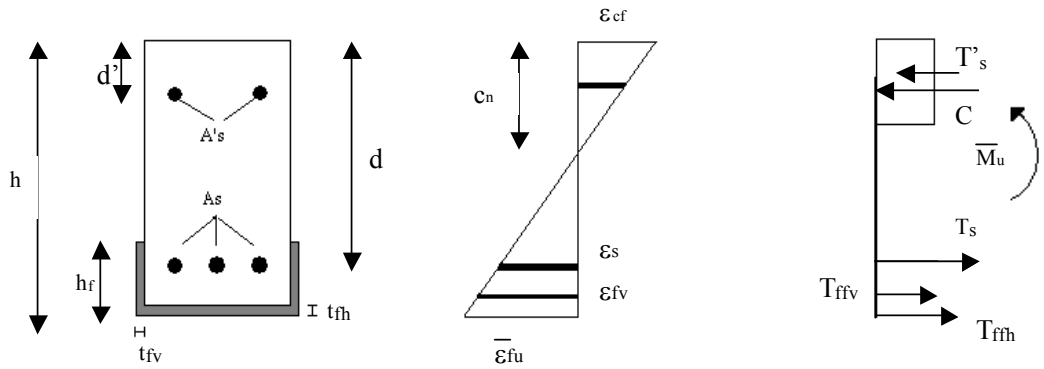

Fig 17. Doubly reinforced section with a wrapped laminate.

The force equilibrium for a doubly reinforced section with a wrapped laminate is:

$$\sum F_x = 0 \Rightarrow \alpha f'_c b c_n - A_s f_y - A_{fv} f_{fv} - A_{fh} f_{fh} + A'_s f'_s = 0 \qquad (49)$$

Substituting equation (40), (42) and (43) into (49), the force equilibrium can be written as:

$$\alpha f'_c b c_n + A'_s f'_s = A_s f_y + b\eta t_{fv} E_f \varepsilon_{fu} + 2 h_f t_{fv} E_f (h - c_n - \frac{h_f}{2}) \qquad (50)$$

The thickness of the vertical wrapped plate can be expressed as

$$t_{fv} = \frac{(\alpha f'_c b c_n - A_s f_y + A'_s f'_s)(h - c_n)}{f_{fu}[\eta b (h - c_n) + 2 h_f (h - c_n - \frac{h_f}{2})]} \qquad (51)$$

The moment equilibrium is taken at the FRP flat laminate as:

$$M_u = \phi M_n = \phi \alpha f'_c b c_n (h - \gamma c_n) - \phi A_s f_y (h - d) - \phi A_{fv} f_{fv} y_{fv} + \phi A'_s f'_s (h - d') \qquad (52)$$

As for singly reinforced section, the point of action of the vertical FRP force y_{fv} is conservatively substituted by $h_f / 2$. Substituting equation (40), (42) and (51) into (52):

$$\frac{M_u}{\phi f_c' b h^2} = \frac{M_n}{f_c' b h^2} = \frac{\alpha c_n (h - \gamma c_n)}{h^2} - \rho_s \frac{f_y}{f_c'} \frac{d}{h}(1 - \frac{d}{h}) + \rho_s' \frac{f_y}{f_c'} \frac{d}{h}(1 - \frac{d'}{h})$$
$$- (\frac{h_f}{h})^2 (\alpha c_n - \rho_s \frac{f_y}{f_c'} d + \rho_s' \frac{f_s'}{f_c'} d) \frac{(h - c_n - \frac{h_f}{2})}{[\eta b (h - c_n) + 2 h_f (h - c_n - \frac{h_f}{2})]} \quad (53)$$

where

$f_s' = f_y$ for yielding of the compression steel

$f_s' = E_s \varepsilon_s'$ for no yielding of the compression steel

As mentioned for singly reinforced wrapped laminates, the 6th degree design equation is very involved to calculate. Instead, equation (50) is used to solve for c_n by assuming values for the FRP area and using equation (52) to solve for $\bar{M}_n$. An analytical linear regression model was developed to calculate the ratio of FRP of wrapped sections for a specific strengthening the moment capacity $\bar{M}_n$ based on an extensive parametric study.

9. Results

9.1 Experimental Verification

A total of 9 FRP-strengthened reinforced concrete beams, with a variety of properties, tested by others are used to verify the equations developed in this paper. All of these beams have failed in FRP rupture and are therefore chosen for comparison.

Table 1. Properties of the beams used in the experimental verification.

Beam (Reference)	FRP type	E_f (GPa)	f_f (MPa)	b_f (mm)	t_f (mm)	A_s (mm^2)	A'_s (mm^2)	f_y (MPa)	f'_c (MPa)	b (mm)	h (mm)	d (mm)	M_n (Nm)
B2[1]	C	400	3000	300	0.17	398	265	340	30	300	400	350	102094
E3[2]	G	13	138	127	1.42	71	0	413	42.5	127	75.8	50.8	3099.3
G3[2]	G	22	190	127	1.22	71	0	413	36	127	75.8	50.8	3332.1
P4[3]	G	11.7	55	150	3	308	308	500	35	150	300	270	44994
E[4]	G	11.7	161	154	4.76	258	0	432	47	152	305	251	60263
L[4]	C	54.4	613	152	1.27	258	0	432	43	152	305	251	59726
P1[5]	G	15.5	170	100	1	168	57	450	37.7	150	150	114	10527
2[6]	C	186	1450	42.6	0.2	33.2	0	517	44.7	76	127	111	3291.3
3[6]	C	186	1450	60.5	0.2	33.2	0	517	44.7	76	127	111	3896.7

[1]Arduini et al (1997), [2]Chajes at al (1994), [3]Djelal and Buyle-Bodin (1996), [4]Ritchie et al (1991), [5]Sharif et al (1994), [6]Trintafillou and Plervis (1992). C = Carbon, G = Glass

The results obtained from the exact solution, equations (20)-(21), (27) or (30) and (31), are compared to those of the approximate solution, equations (37)-(39), and to the experimental values, Fig. (18) and (19). It can be seen from Figs. (18) and (19) that the comparison yields an almost perfectly matching results for c_n and ρ_f. This provides confidence in the accuracy of the exact equations and in the validity of the assumptions adopted for the approximate solution, for the range of experimental data examined.

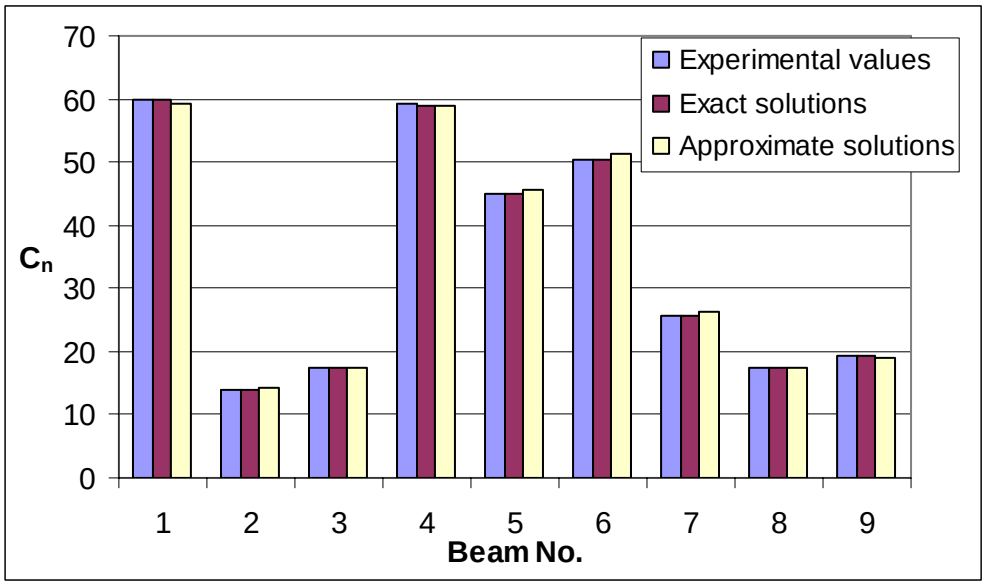

Fig. 18 Experimental verification for c_n value

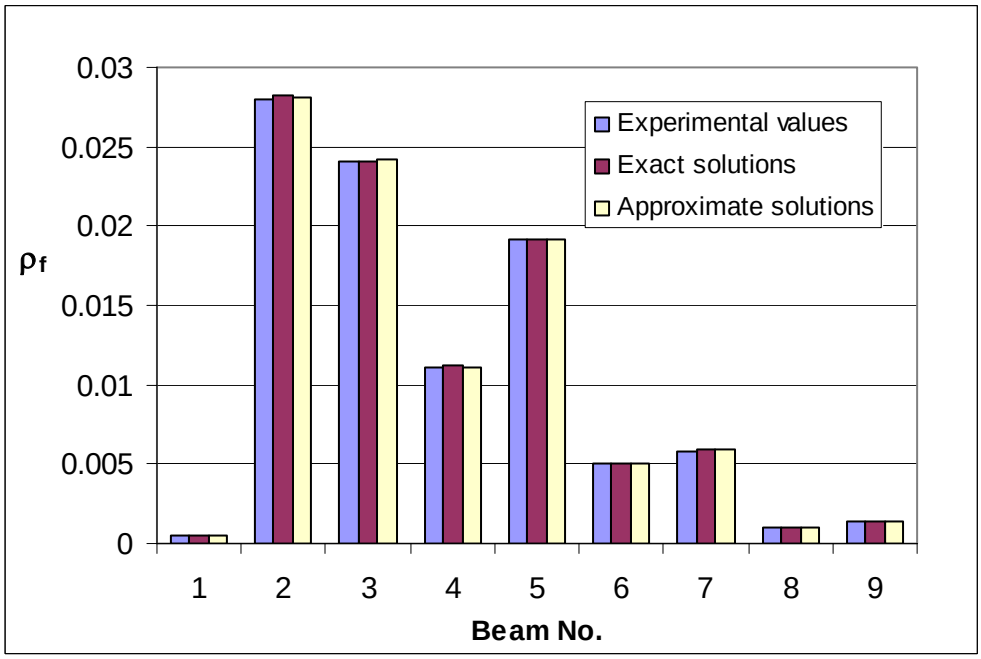

Fig. 19 Experimental verification for ρ_f value

9.2 Parametric study for flat laminates

To examine the relevance of the approximate solution to the exact one, an extensive parametric study is conducted. This study was also done to investigate the effects of the design variables on the results. These variables are the cross section dimensions, tension steel reinforcement ratio, compression steel reinforcement ratio, strengthening design moment, concrete material properties, steel material properties, FRP material type and properties, as shown in Fig. 20.

For every set of fixed variables, the FRP ratio is set to zero first and the moment of the unstrengthened beam is calculated (M_n). The moment of strengthened beam ($\bar{M}_n$)is then increased by $0.1M_n$ steps ($1.1M_n$, $1.2M_n$,…) and the corresponding FRP ratio is calculated until the mode of failure changes from FRP rupture to concrete crushing. The steel ratio is varied between its minimum and maximum values specified by (ACI 318-99). Ratios close to the maximum limit always yields concrete crushing failure mode. Accordingly, the tension steel ratio is limited to three values varying from minimum to moderately high levels (0.0045, 0.00875, and 0.013). The compression steel is varied between zero (singly reinforced section), a low ratio (0.002) and a high ratio (0.01). The two FRP materials examined are Glass FRP (GFRP) and carbon FRP (CFRP). The GFRP is assumed to have a modulus of elasticity of E_{GFRP} = 45 GPa and a strength of f_{GFRP} = 400 MPA. The CFRP properties are assumed to be E_{CFRP} = 400 GPa and f_{CFRP} = 3000 MPa.

The results are plotted in terms of the relationship between the ratio of strengthened to unstrengthened moment capacity $\bar{M}_n/M_n$ vs. the FRP ratio. These results were studied to investigate the effects of changing the variables.

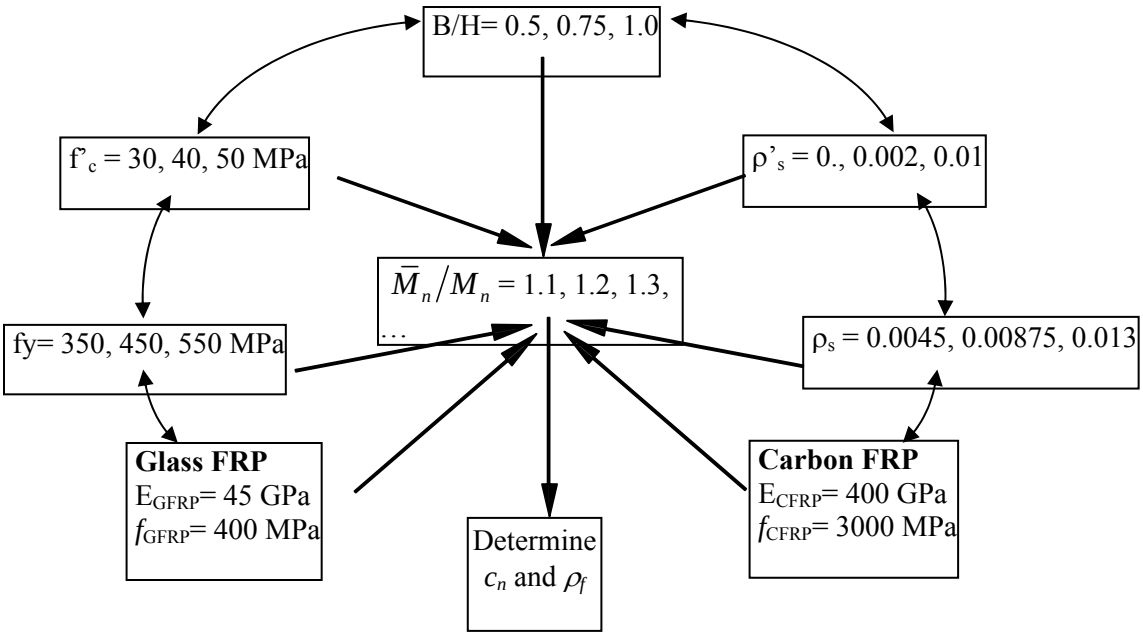

Fig 20 Variation of design variables in the parametric study

A sample of listing of the design variables used in the parametric study for flat is presented in appendix A.

9.2.1 Effect of varying parameters

The steel ratio, B/H ratio and FRP material type and properties are the main parameters that are expected to have noticeable effects on the strengthening design of the beam. These parameters have therefore been closely examined.

Effect of tension steel ratio-To study the effect of ρ_s, it is varied as mentioned above (0.0045, 0.00875 and 0.013). The f'$_c$ = 30 MPa and f_y = 350 MPa, are the same for all three GFRP reinforced sections with a compression steel ratio ρ's = 0.01. The effect of ρ_s is illustrated in Fig 21. It can be seen that there is a straight-line relationship between the FRP ratio and moment capacity ratio for each fixed steel ratio regardless of the B/H ratio used. Accordingly, it is concluded that the steel ratio clearly affects the slope of the linear relationship generated. On the other hand, the FRP ratio does not seem to be affected by changing the section dimension ratio (B/H).

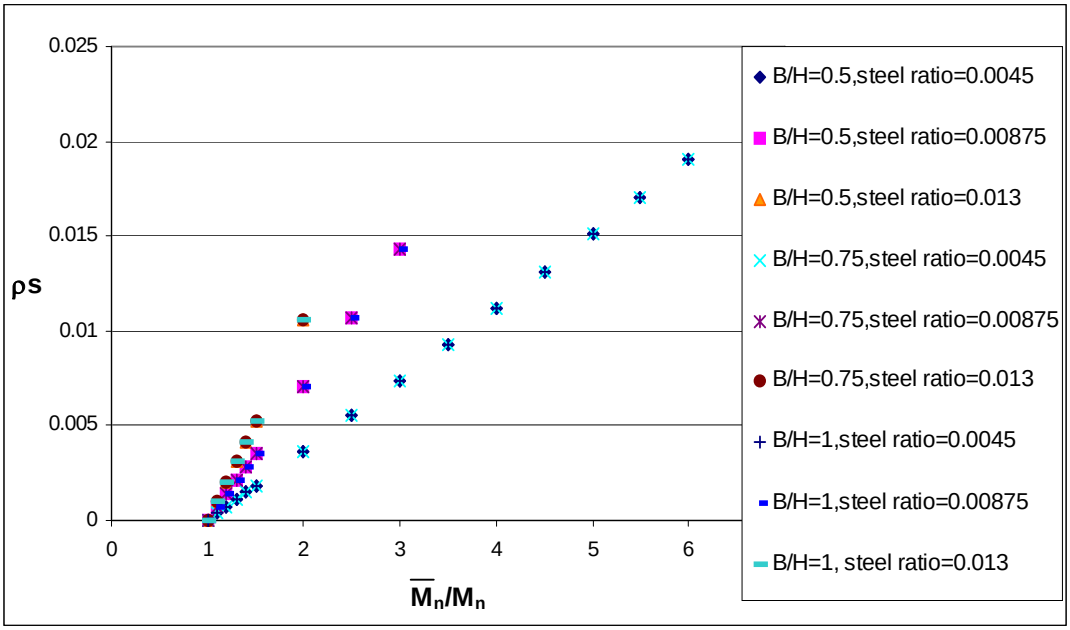

Fig. 21 The effects of varying tension steel ratio and B/H

Effect of compression steel ratio- the parameter of compression steel is chosen to determine whether it has an effect on the amount of FRP ratio. To determine this effect, the compression steel is varied between 0 (singly reinforced section) a lower amount of reinforcement 0.002, and a high value of compression steel reinforcement 0.01. To illustrate this effect, the section chosen has a B/H=1, GFRP plate with ρ_s = 0.0045 as typical values. The variations of the compression steel are illustrated in Fig. 22. Fig. 22 clearly shows that the ratio of compression steel has no effect on the solution since all of its three values yielded points along the same straight line.

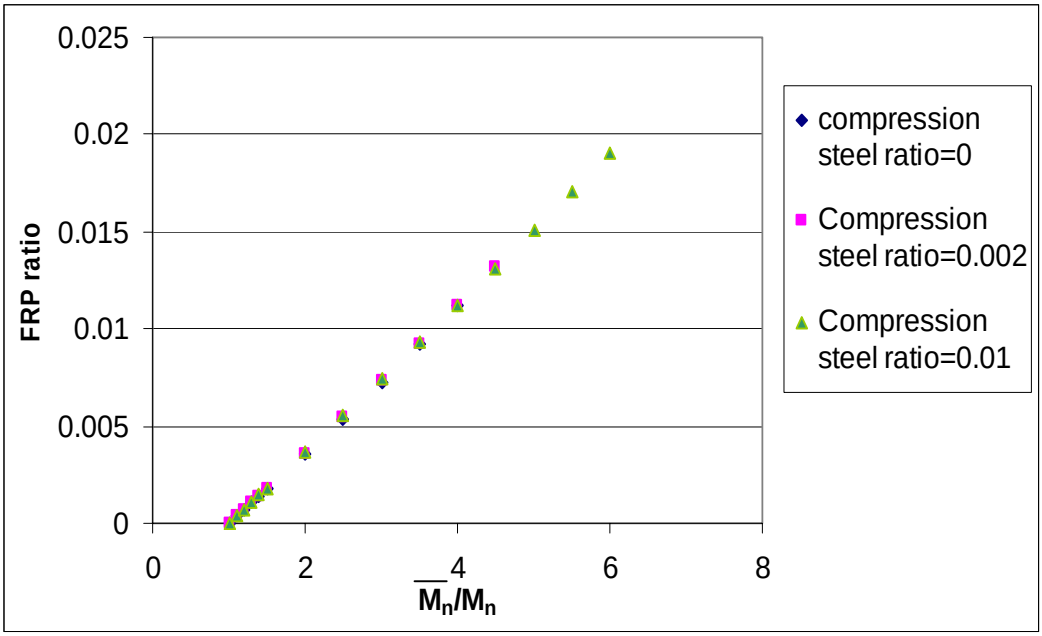

Fig. 22 The effect of varying ρ'$_s$

Effect of different FRP materials- The two strengthening materials used in this study are Glass and Carbon FRP. Two sections are selected with B/H=0.5 and B/H=1 for both cases of materials. The steel ratio chosen in both cases is 0.0045. This variation is demonstrated in Fig. 23. Fig. 23 shows that the solution is different for different FRP materials regardless of the B/H ratio. However, the results have still yielded linear variation for the same FRP material examined. Accordingly, it is important to consider this factor when designing for ρ_f .

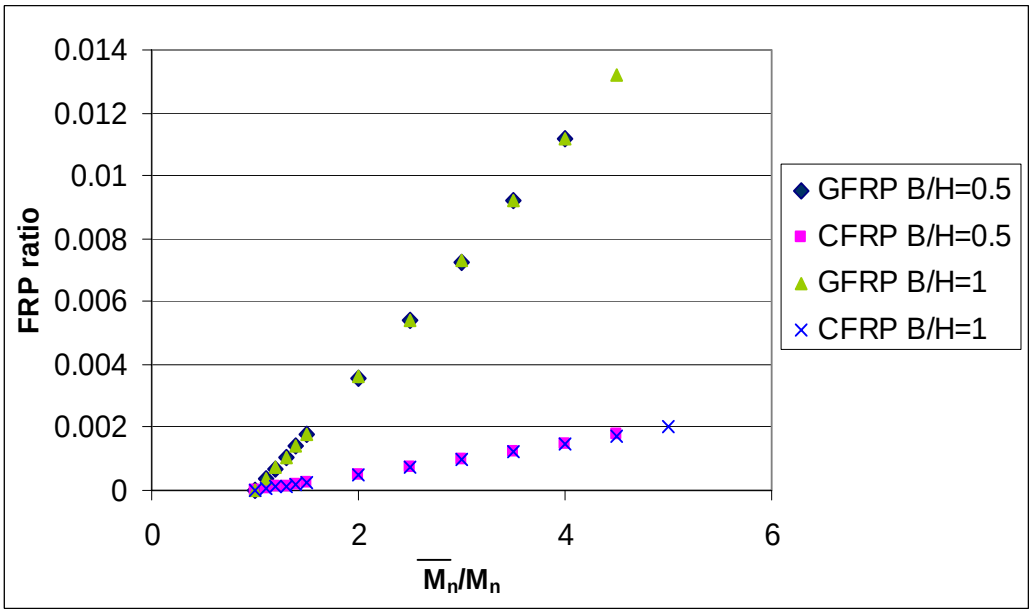

Fig. 23 The effects of varying FRP type and B/H

Effect of f'c- To study the influence of the compressive strength of concrete on the solution, three values of f'c (30, 40, 50 MPa) are selected. To separate the effect of this parameter only, a B/H=1 and ρ_s=0.00875 for a CFRP singly reinforced section are fixed as typical values and the results are plotted for $\overline{Mn}/Mn$ against the FRP ratio of the section. According to Fig. 24, the compressive strength of concrete has a negligible effect on the variation of the FRP ratio and the linear trend of results is still sustained.

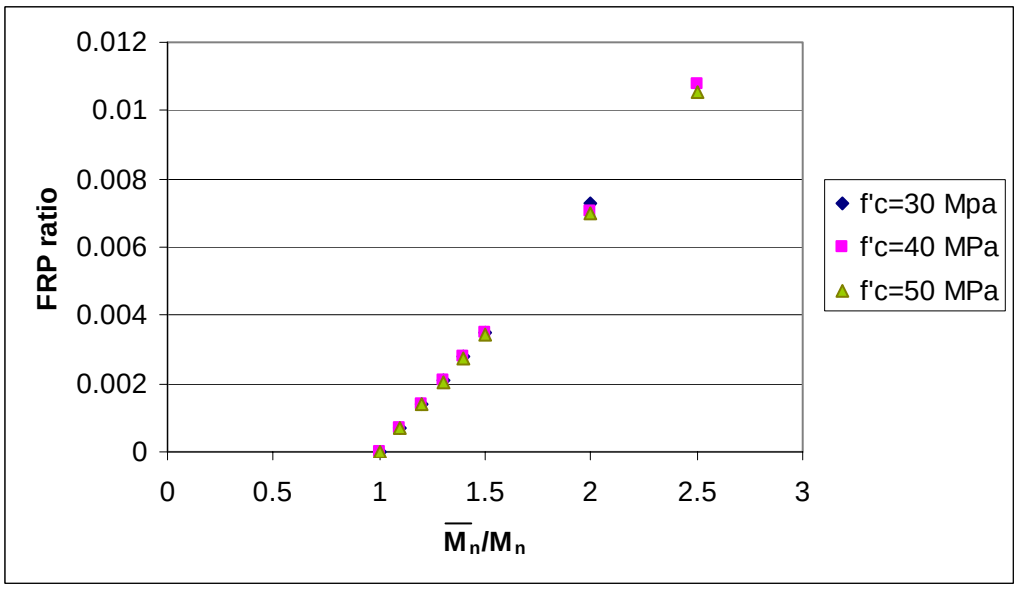

Fig. 24 The effects of varying f'c.

Effect of f_y- The last parameter studied is the yield strength of steel f_y, where three values of fy are selected (350, 450, 550 MPa). The section B/H=0.75 and ρ_s=0.0045 for a CFRP doubly reinforced section (with ρ'_s=0.002) is chosen as typical values, while the yield strength of steel f_y is varied. The results are plotted for $\overline{Mn}/Mn$ against the FRP ratio of the section in Fig 25. The results show that the variation of f_y has an influence on the ratio of FRP. Accordingly, it is important to consider this factor when designing for ρ_f .

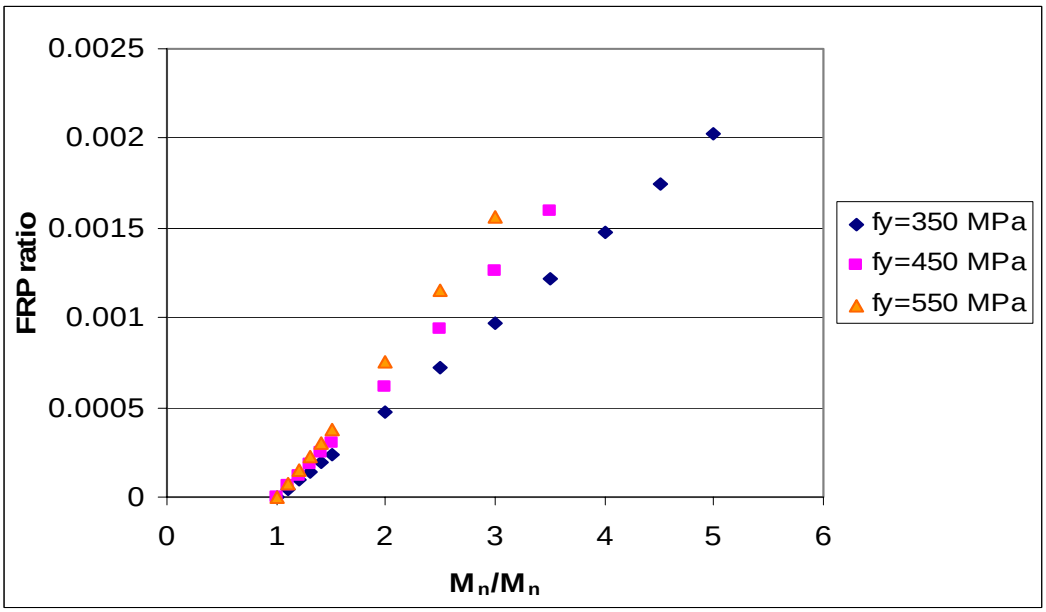

Fig 25. The effects of varying f_y

9.2.2 Normalization and regression analysis

The parametric study has yielded the parameters which have an effect on the results to be the steel ratio (ρ_s), the yield strength (fy) and the different FRP material chosen. These effects are seen to be simply in terms on changing the slope of the linear trend obtained for the three parameters mentioned. As discussed earlier, there are two factors changing with the different FRP material, the elastic modulus and strength. It is important to take into consideration whether only one of these factors has an effect on the results or both factors affect the variation.

By normalizing the ratio of FRP which is calculated from equations (12) or (21), by the factors influencing the results, a unique linear variation is obtained, which can be used for any singly or doubly reinforced rectangular section. The ρ_f normalizing factor is non-dimensional and is referred to in this paper as the reinforcement strength ratio λ.

$$\lambda = \frac{\rho_f f_{fu}}{\rho_s f_y} \qquad (54)$$

Normalizing all the FRP ratios calculated for the parametric study to obtain the corresponding λ values and plotting it against $\overline{M_n}/M_n$, an almost perfect straight line is generated with $R^2 = 0.9994$, for the 1500 data points examined, Fig. 26. This presents an excellent contribution of this paper since a single linear function may be effectively used to replace the exact or approximate solutions. It can be further used to solve analysis problems as well.

$$\lambda = 0.9527\overline{M_n}/M_n - 0.9691 \qquad (55)$$

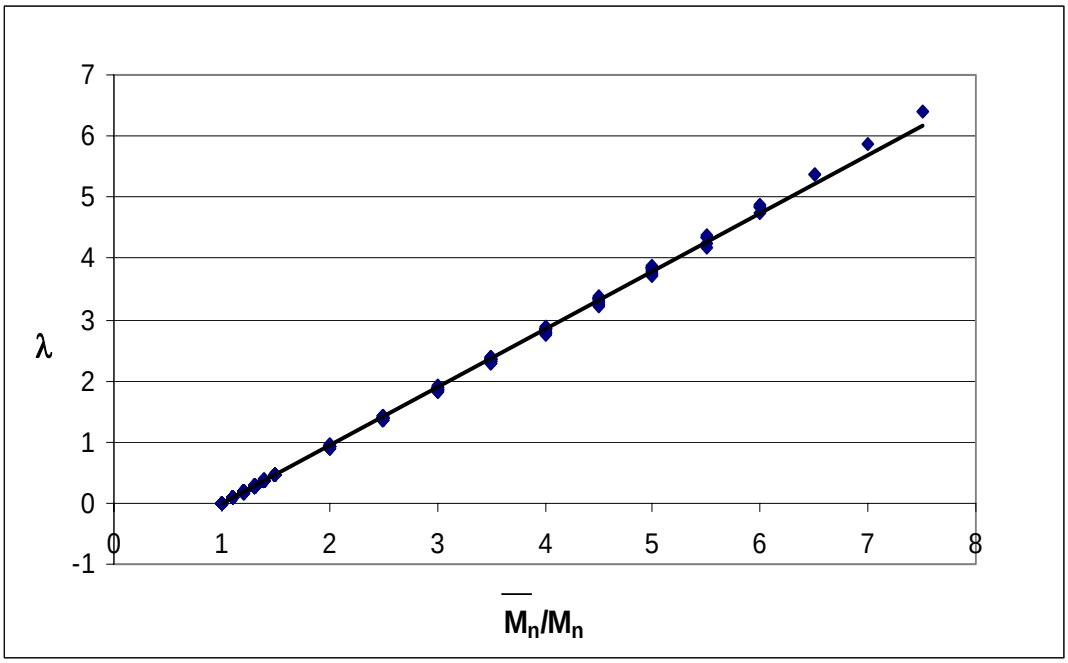

Fig. 26 The unique linear regression design equation.

Fig 26 also shows that all the data with the same $\overline{M_n}/M_n$ give the same λ.

9.2.3 Comparison of regression equation and exact solutions

To verify the accuracy of the linear regression expression, 70 different examples of the parametric study were solved again using the exact solution and the regression equation. The ratios of FRP calculated from both solutions are compared and plotted in Fig. 27. The comparison clearly presents an almost perfect match of the results. Detailed input values and results of the 70 examples solved for flat laminates are presented in appendix B.

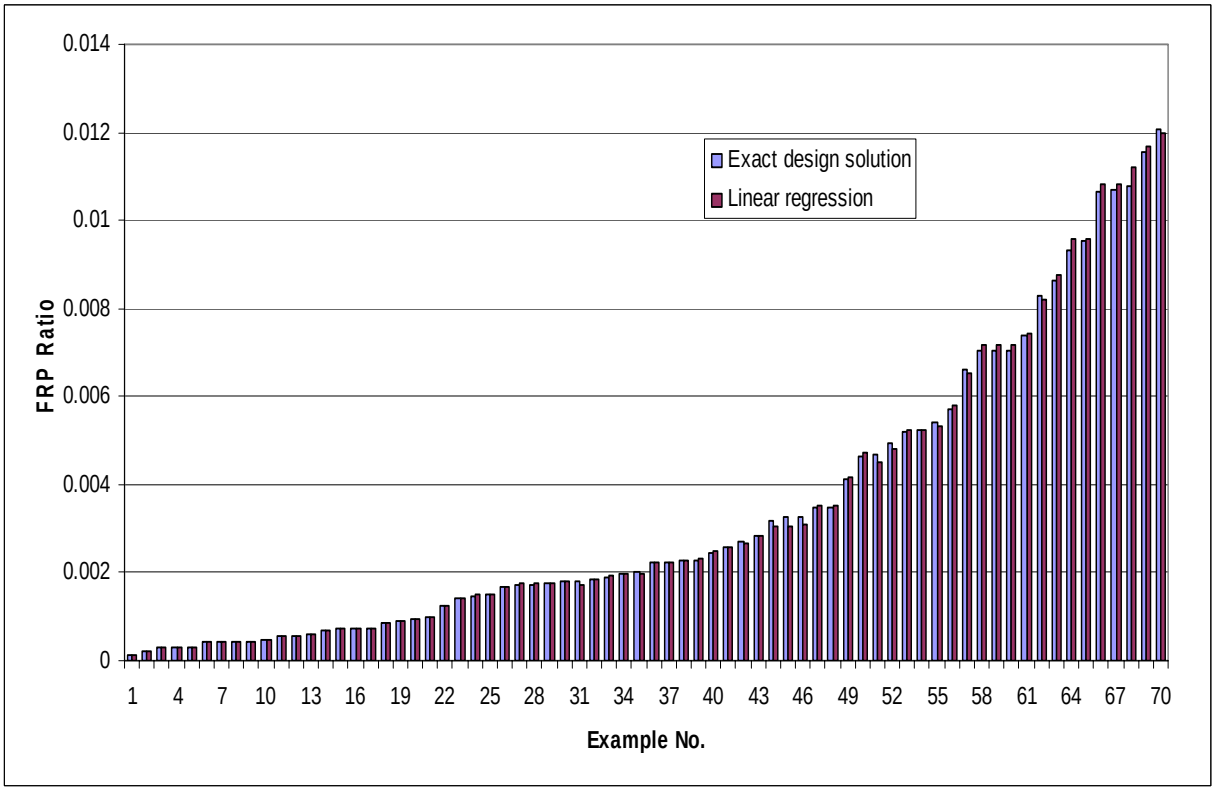

Fig. 27 Comparing linear regression and exact design solution for flat laminates

9.3 Parametric study for wrapped laminates

The same parametric study performed for the flat laminates is conducted for the wrapped flexural FRP reinforcement. Since the design equations presented earlier are too complicated to use; the analysis equations are used to generate the needed points for the parametric study by assuming the FRP ratio and solving for $\overline{M}_n / M_n$.

The design parameters in this parametric study are varied the same way done for flat laminates, see Fig. 20. The tension steel ratio is varied between 0.0045 and 0.013.. Three compression steel ratios are selected to be zero (singly reinforced section), a low ratio (0.002) and a high ratio (0.01). The two FRP materials examined are Glass FRP (GFRP) and Carbon FRP (CFRP). The ratio of the flat thickness to the side FRP thickness (η) is varied between 1 (which gives the same thickness for horizontal and vertical sheets), 1.5 and 2.

A sample of listing of the design variables for the wrapped laminates used in the parametric study is presented in appendix C.

Example 2: ISIS Canada Rupture Analysis Examples

According to the guidelines given by the ISIS Canada design manual (2001) for strengthening reinforced concrete structures with externally bonded fiber-reinforced polymers, different material resistance factors ϕ are implemented. In this manual, there is a resistance factor for concrete, steel and FRP. The resistance factors for concrete (ϕ_c=0.6) and steel (ϕ_s=0.85) are directly adopted from the CSA standard A23.3-94 for structures other than bridges. The ISIS Canada manual (2001) seems to suggest a value of ϕ_{frp}=0.75 for CFRP and to propose a range of values from 0.6 to 0.76. Accordingly, the present exact design equations will be slightly changed to incorporate these ϕ factors in order to make a direct comparison with two examples given in these guidelines.

The force equilibrium according to the ISIS Canada manual is:

$$\sum F_x = 0 \Rightarrow \phi_c \alpha f_c' b c_n + \phi_s A_s' f_s' - \phi_s A_s f_y - \phi_{frp} A_f f_{fu} = 0$$

The moment equilibrium taken at the FRP plate level gives:

$$M_u = \phi_c \alpha f_c' b c_n (h - \gamma c_n) - \phi_s A_s f_y (h - d) + \phi_s A_s' f_s' (h - d')$$

$$M_u = \phi_c \alpha f_c' b c_n (h - \gamma c_n) - \phi_s A_s f_y (h - d) + \phi_s A_s' f_s' (h - d')$$

which may be re-arranged as:

$$\frac{M_u}{\phi_c f_c' b h^2} = \frac{\alpha c_n (h - \gamma c_n)}{h^2} - \frac{\phi_s}{\phi_c} \rho_s \frac{f_y}{f_c'} \frac{d}{h^2} (1 - \frac{d}{h}) + \frac{\phi_s}{\phi_c} \rho_s' \frac{f_s'}{f_c'} \frac{d}{h^2} (1 - \frac{d'}{h})$$

By Collecting all the terms that do not include the neutral axis (c_n) under one variable name, the equation above can be written as:

$$Q_u'' - \frac{\alpha c_n (h - \gamma c_n)}{h^2} - \rho' s \frac{\varepsilon' s \, E' s}{f' c} \frac{d}{h} (1 - \frac{d'}{h}) = 0$$

where

$$Q_u'' = \frac{M_u}{\phi_c f_c' b h^2} - \frac{\phi_s}{\phi_c} \rho_s \frac{f_y}{f_c'} \frac{d}{h} (1 - \frac{d}{h})$$

Substituting equations (12), (13) and (24) into the equation above, the exact solution for calculating the neutral depth c_n for singly reinforced sections becomes:

$$A \frac{c_n}{h} + B (\frac{c_n}{h})^2 + D (\frac{c_n}{h})^3 + E (\frac{c_n}{h})^4 + F (\frac{c_n}{h})^5 - 12 Q_u'' \varepsilon' c = 0$$

9.3.1 Normalization and regression analysis

It is very interesting to observe the same linear trends generated for flat laminates to equally hold for the wrapped ones. By normalizing the FRP ratio the same way made for the flat laminates, 826 data points of this parametric study establish an almost perfect straight line with $R^2 = 0.9985$ for the wrapped sections as shown in Fig. 28. The resulting linear regression equation is:

$$\lambda = 0.971\overline{M}_n / M_n - 0.9844 \qquad (56)$$

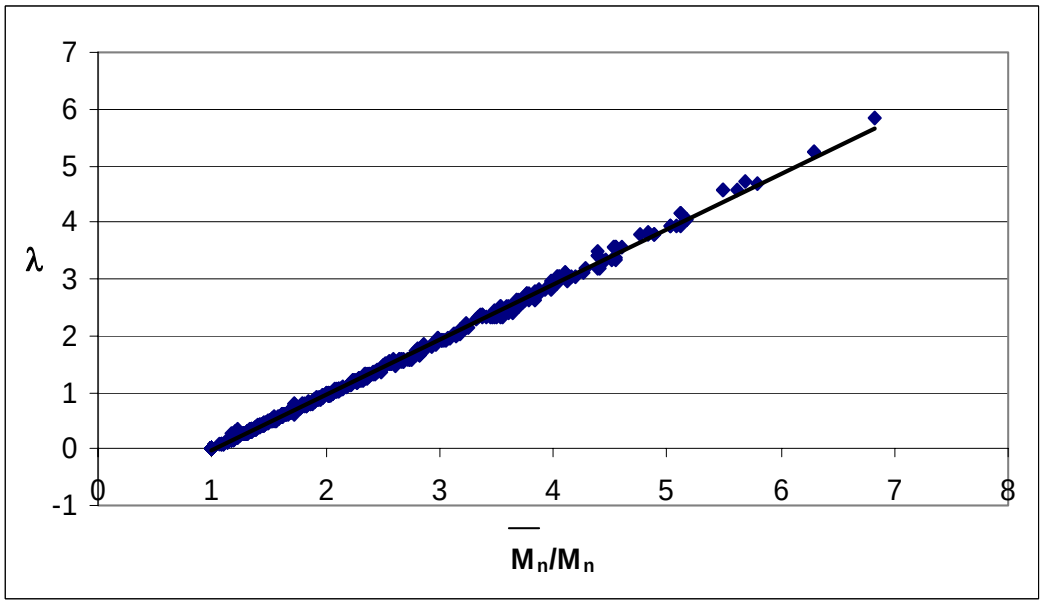

Fig. 28 Linear regression design/analysis equation for wrapped laminates

9.3.2 Comparison of regression and exact solutions

To verify the accuracy of the linear regression solution, 70 different examples of the parametric study, of the wrapped section, were solved again using the exact solution and the regression equation. The FRP ratios calculated from both solutions are compared and plotted in Fig 29. The comparison clearly presents an almost perfect match of the results. Detailed input values and results of the 70 examples solved for flat laminates are presented in appendix D.

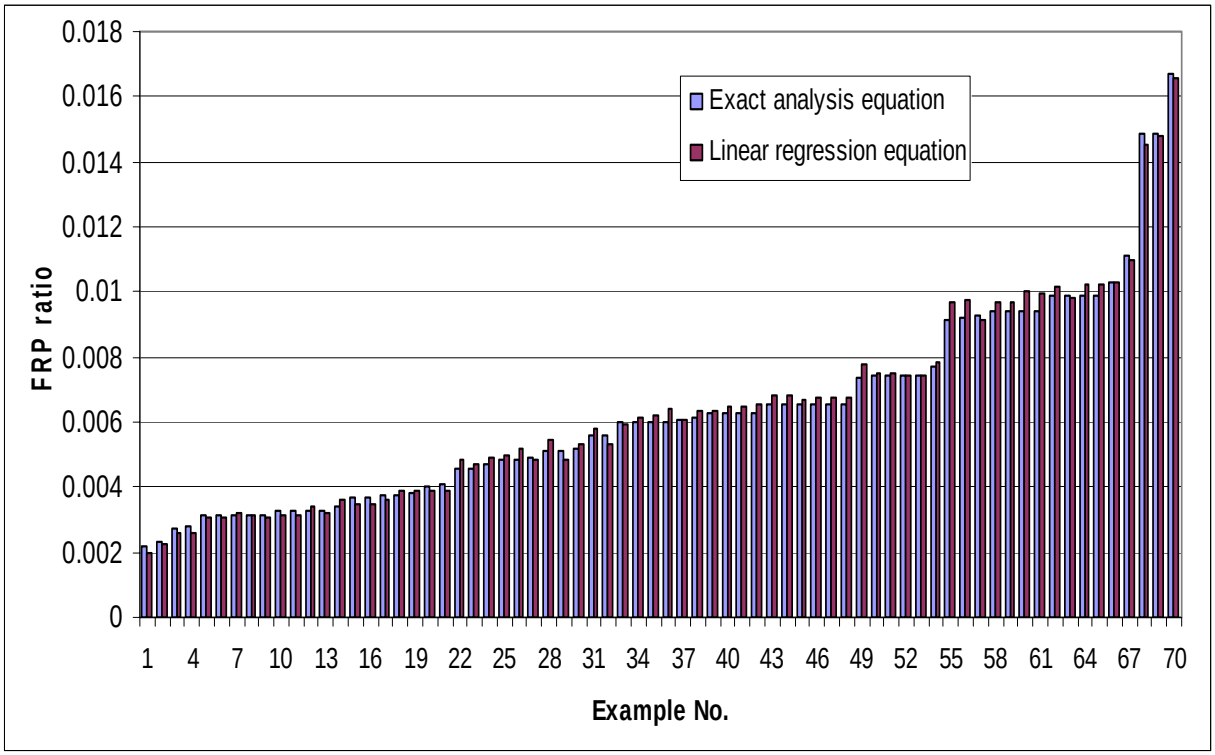

Fig. 29 Comparing linear regression and exact design solution for wrapped laminates

9.4 Flat and wrapped section

All data points from the parametric study for flat laminates and wrapped laminates can be put in the same diagram, as in Fig 30.
It is interesting to see that the lines are very close and therefore can be expressed with one equation for this line.
An almost perfect straight line with $R^2 = 0.9987$ is expressed in equation (57) for a straight line which can be use for both flat and wrapped laminates.

$$\lambda = 0.9626\,\overline{M}_n / M_n - 0.976 \qquad (57)$$

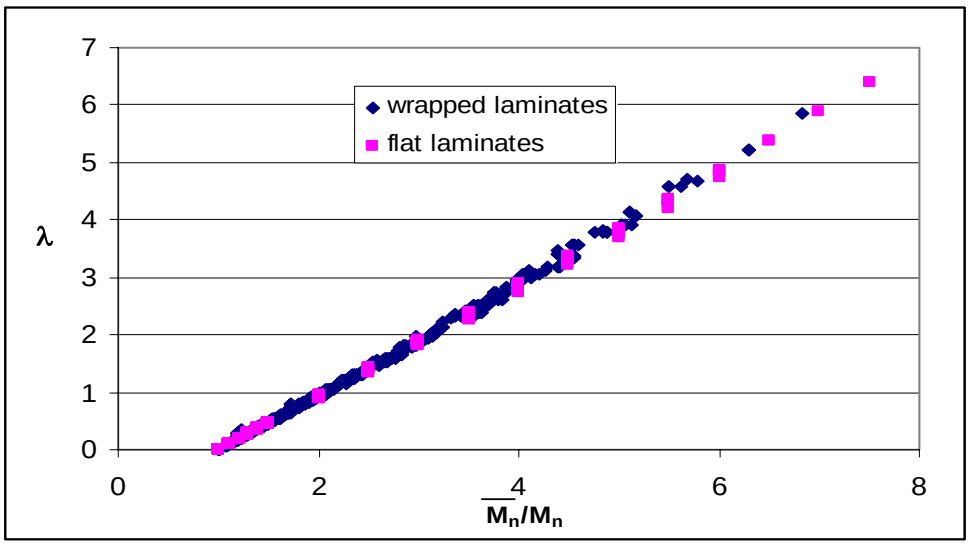

Fig 30. Linear regression design equation for flat and wrapped laminates

It is interesting to show the equal trend for both the cases with flat and wrapped laminates. It is however; more appropriate to chose the separate equations (equation (55) for flat laminates and equation (56) for wrapped laminates) when calculating the ratio of FRP reinforcement, since the separate equations were generated for the design variable for the representative cases.

10. Examples:

Example 1: Flat and wrapped laminates

An example from the parametric study is picked to show the design of flat and wrapped laminates. The example is a singly reinforced GFRP section with the width, b = 300mm and the height h = 400 mm. The steel ratio ρ_s =0.013, the strength of the concrete f_c' =50 MPa and the strength for the steel f_y =350 Mpa.

For the wrapped section two examples are selected, one with small vertical reinforcement height h_f =20 mm, and one with longer vertical reinforcement height h_f =60 mm. The η=1.5 for these examples.

The ratio of strengthened to unstrengthened moment capacity is chosen $\overline{M_n}/M_n$ =1.5.

Flat laminates

By using equation 56 for flat laminates

λ = 0.46

The FRP ratio for this section calculated with linear regression

ρ_f = 0.005232 which gives a thickness of t =1.818 mm.

This gives an error of 0.77 % from the exact solution.

Wrapped laminates

By using equation 57 for wrapped laminates

λ = 0.472

The FRP ratio for the wrapped section calculated with linear regression

ρ_f = 0.00537

h_f =20 mm

The horizontal thickness t_{fh} =1.615 mm. and vertical thickness t_{fv} =1.08 mm.

This gives an error of –2.67 % from the exact solution.

h_f =60 mm

The horizontal thickness t_{fh} =1.364 mm. and vertical thickness t_{fv} =0.909 mm.

This gives an error of 1.55 % from the exact solution.

The same equation for doubly reinforced sections with yielding of compression steel is:

$$A'\frac{c_n}{h} + B'(\frac{c_n}{h})^2 + D'(\frac{c_n}{h})^3 + E'(\frac{c_n}{h})^4 + F'(\frac{c_n}{h})^5 - 12Q_u''\varepsilon'_c = 0$$

and for doubly reinforced sections with no yielding of compression steel is:

$$A'\frac{c_n}{h} + B'(\frac{c_n}{h})^2 + D'(\frac{c_n}{h})^3 + E'(\frac{c_n}{h})^4 + F'(\frac{c_n}{h})^5 - Q_u''G'' = 0$$

where

$$G'' = \frac{\phi_s}{\phi_c}\rho'_s\frac{\varepsilon'_s E'_s}{f'_c}\frac{d}{h}(1-\frac{d'}{h})$$

The ratio of FRP reinforcement is simply calculated for the doubly reinforced sections by rearranging the force equilibrium equation above after determining c_n:

$$\rho_f = \frac{\phi_c}{\phi_{frp}}\alpha\frac{f'_c}{f_{fu}}(\frac{c_n}{h}) - \frac{\phi_s}{\phi_{frp}}\rho_s\frac{f_y}{f_{fu}} + \frac{\phi_s}{\phi_{frp}}\rho'_s\frac{f_y}{f_{fu}}$$

Examples 4.2 and 4.5, in the Canadian guidelines, illustrate the analysis approach used to strengthen a singly and doubly reinforced section with CFRP. The above equations will be used here to solve these two examples using a direct design approach and compare the results with those of ISIS Canada manual calculations.

Data

Design Example 4.2

Section properties		Composite properties	
h=	600mm	b_f=	100mm
b=	400mm	f_{fu}=	2402.5MPa
f'_c=	45MPa	E_f=	155GPa
A'_s=	0	A_f=	120mm^2
A_s=	1500mm^2		
d=	546mm		
d'=	0		

Design Example 4.5

Section properties		Composite properties	
h=	600mm	b_f=	100mm
b=	400mm	f_{fu}=	2402.5MPa
f'_c=	45MPa	E_f=	155GPa
A'_s=	400	A_f=	120mm^2
A_s=	1500mm^2		
d=	546mm		
d'=	54mm		

Results
Design example 4.2:
Canadian guideline: $A_f = 120$ mm^2, $c_n = 100$ mm
Calculations based on the present exact solution: $A_f = 115$ mm^2, $c_n = 89.36$ mm

Design example 4.5:
Canadian guideline: $A_f = 120$ mm^2, $c_n = 86.4$ mm
Calculations based on the present exact solution: $A_f = 116$ mm^2, $c_n = 83.57$ mm

The results from the Canadian analysis examples and the present design solution are close to each other. However they are not exactly matching due to the fact that the expressions used for α (α_1 in the manual) and γ (β_1 in the manual) by the ISIS Canadian guidelines are those developed for concrete crushing ($\varepsilon_{cu} = 0.003$). In this case, $\varepsilon_{cf} = 0.0027$ was found for the singly reinforced sections and $\varepsilon_{cf} = 0.00256$ was determined for the doubly reinforced section, which clearly renders different α and γ values.

11. Conclusions

The objective of this study was to develop direct solution procedure to design externally bonded FRP reinforcement for the rupture mode of failure, considering both flat and wrapped laminates. For the flat reinforcement, exact 5^{th} degree polynomial expression was derived for the location of neutral axis, from which the ratio of FRP is directly obtained. By introducing relevant approximations, 3^{rd} degree polynomial expressions were established yielding easier solution yet equally accurate results. An extensive parametric study was conducted to qualify the accuracy of the approximate solution relative to the exact results. This study has revealed a unique linear regression equation between the ratio of tension reinforcement stiffness (λ) and the ratio of strengthened to unstrengthened moment capacity. This simpler linear solution was further examined against the exact solution and was seen to yield excellent match.

For the wrapped laminates, the exact expression for designing the section was very lengthy and involved. Therefore, it was not used to generate any results. The analysis expressions were used, instead, to generate data points for the parametric study. This study showed that the same unique linear relationship for flat laminate can be generated for the wrapped laminates. The result for the wrapped reinforcement is not as accurate as for the flat laminates. This simple linear solution was further examined against the exact analysis solution and was seen to yield a very good match. Since the wrapped laminate design included extra variables like the height of the side FRP and the ratio of flat to side FRP thickness, the linear regression solution in this case is expected to deviate from the exact solution more so than the case of flat laminates. The average percentage of deviation was found to be 1.5% based on 70 data points for the flat laminates. The greatest deviation was 5.9 % for the following design parameters. On the other hand, the average percentage of deviation was found to be 3.2 % based on 70 data points for the wrapped laminates. The largest difference in this case was 8.43 % for the following design variables.

References

ACI 440R-96 (1996), State-of-the Report on Fiber Reinforced Plastic (FRP) Reinforcement for Concrete Structures, ACI Committee 440, American Concrete Institute, Farmington Mills, MI 68 pp.

ACI 440.2R-02 (2002), Guide for the Design and Construction of Externally Bonded FRP Systems for Strengthening Concrete Structures, ACI Committee 440, American Concrete Institute, Farmington Mills, MI, 45 pp.

Arduini, M.; Nanni, A., "Behavior of Precracked RC Beams with Carbon FRP Sheets" *Journal of Composites for Construction*, ASCE Vol. 1, No.2, 1997, pp.63-70.

An, W.; Saadatmanesh, H.; Ehsani, R., "RC Beams Strengthened with FRP plates " *Journal of Composite for Construction*, ASCE, Vol. 117, No.11, November, 1991.

Bakis, C. E., Bank, L. C., Brown, V. L., Cosenza, E., Davalos, J. F., Lesko, J. J., Machida, A., Rizkalla, S. H. and Triantafillou, T. C., Fiber-Reinforced Polymer Composites for Construction—State-of-the-Art Review, *Journal of Composites for Construction*, ASCE, Vol. 6, No. 2, 2002, pp. 73-87.

Bonacci, J.F.; Maalej, M., "Behavioral Trends of RC Beams Strengthened with Externally Bonded FRP" *Journal of Composite for Construction*, ASCE, Vol. 5, No.2, May, 2001.

Chajes, M.J.; Thomson, T.A.; Januszka T.F., "Flexural Strengthening of Concrete beams Using Externally Bonded Composite Materials" *Journal of Construction and Building Materials*, V.8, No.3, 1994, pp. 191-201.

Charkas, H.; Rasheed, H.A; Melhem, H., "Rigorous Procedure for Calculating Deflections of Fiber-Reinforced Polymer-Strengthened Reinforced Concrete Beams", *ACI Structural Journal*, Vol.100, No. 4, May-June, 2004.

Dejke V. (2001), "Durability of FRP Reinforcement in Concrete", Literature review and Experiments. Licentiate thesis, Chalmers, Göteborg. 211 pp.

Djelal, C., David, E., and Buyle-Bodin, F. (1996). "Utilisation de plaques en composite pour la reparation de poutres en beton arme endommagees." Proc. *2nd Conf. On Advanced Compos. Mat. In Bridges and Struct.* M. El-Badry, ed., Canadian Society for Civil Engineering, Ottawa, 581-588.

Fardis, M. N. and Khalili, H. H., Concrete encased in fiberglass-reinforced plastic," ACI Structural Journal, Title No. 78-38, Nov.-Dec. 1981, pp. 440-446.

Fardis, M. N. and Khalili, H. H., FRP-encased concrete as a structural material, Magazine of Concrete Research, Vol. 34, No. 121, Dec. 1982, pp. 191-202.

ISIS Canada (2001a) “Design Manual 4: Strengthening Reinforced Concrete Structures with Externally-Bonded Fiber Reinforced Polymers,” The Canadian Network of Centers of Excellence on Intelligent Sensing for Innovative Structures, University of Manitoba, Winnipeg, Manitoba, Canada, Sept. 2001, 207p.

Mc Gregor, James G., ”Reinforced concrete, Mechanics and Design”, Third Edition, Prentice Hall, Upper Saddle River, NJ. 1995. 939 pp.

Meier, U., Brülckensanierung mit Hochleistungs-Faserverbundwerkstoffen, *Material und Technik,* Vol. 15, 1987, pp. 125- 128.

Mårtensson, Annika, “Betongkonstruktioner”, Avdelningen för konstruktionsteknik, Lunds Tekniska Högskola, Lunds Universitet, Lund, February 2000. (Swedish)

Park, R., and Paulay, T., *Reinforced Concrete Structures*, John Wiley & Sons, Inc., New York, 1975, 769 pp.

Ritchie, A.P.; Thomas, D.A.; Lu, L.; Conelly, G.M., “External Reinforcement of Concrete Beams Using Fiber Reinforced Plastics” *ACI Structural Journal*, V.88, No.4, July 1991.

Rasheed, H.A.; Pervaiz S., “Closed form equations for FRP flexural strengthening design of RC beams”, *Composites part B: Engineering*, Vol.34, pp.539-550, 2003

Sharif, A.; Al-Sulaimani G.J.; Basunbul I.A.; Baluch M.H. and Ghaleb, B.N. (1994). “Strengthening of Initially Loaded Reinforced Concrete Beams using FRP Plates”. *ACI Structural Journal*, 91(2), 160-168.

Triantafillou R.C. and Plervis, N. (1992). “Strengthening of RC beams with epoxy-bonded fiber-composite materials”. *Mat. and Struct.*, 25, 201-211.

Appendix A

Below is a sample of listing of the design variables used in the parametric study for flat laminates. This listing includes 468 data out of the 1500 ones used for this paper. Due to space limitations, it was not possible to report all data sets.

FRP	***B/H***	ρ'_S	f'_c	f_y	ρ_s	$\overline{M_n}/M_n$	***t (mm)***	ρ_f*(exact)*	ρ_f*(approx.)*	***Cn*** *(exact)*	***Cn*** *(approx)*
Glass	0,5	0,01	30	350	0,0045		0	0	0	45,49163	45,539016
						1	0,12808	0,000366	0,00036058	46,67077	46,653472
						1,1	0,2563	0,000732	0,000725	47,83557	47,746876
						1,2	0,38467	0,001099	0,00108965	48,98694	48,820594
						1,3	0,51319	0,001466	0,00145451	50,12575	49,875521
						1,4	0,64186	0,001834	0,00181959	51,2528	50,912491
						1,5	1,28763	0,003679	0,00364844	56,73652	55,85321
						2	1,93777	0,005536	0,00556211	62,02304	61,50798
						2,5	2,59277	0,007408	0,0074464	67,17607	67,307023
						3	3,25319	0,009295	0,00934083	72,25095	72,855076
						3,5	3,91977	0,011199	0,01124505	77,3007	78,172658
						4	4,59346	0,013124	0,01315882	82,38179	83,277821
						4,5	5,27559	0,015073	0,01508188	87,56151	88,186431
						5	5,96822	0,017052	0,01701399	92,93053	92,91252
						5,5	6,67467	0,01907	0,0189549	98,62886	97,468573
						6	6,8	0,0196	0,0195	100,28	98,69
					0,00875		0	0	0	56,85204	55,955333
						1	0,24283	0,000694	0,00071	58,8486	57,873045
						1,1	0,4863	0,001389	0,00141152	60,8214	60,136559
						1,2	0,73043	0,002087	0,0021147	62,77369	62,361387
						1,3	0,97525	0,002786	0,00281932	64,70851	64,548237
						1,4	1,2208	0,003488	0,00352538	66,62879	66,698391
						1,5	2,46048	0,00703	0,00707656	76,1097	76,938928
						2	3,72441	0,010641	0,01066142	85,65784	86,419859
						2,5	5,02283	0,014351	0,01427815	95,76654	95,242856
					0,013		0	0	0	67,256	67,396
						1	0,359	0,001028	0,00107	70,032	70,452
						1,1	0,721	0,00206	0,002107	72,794	73,432
						1,2	1,085	0,003099	0,003146	75,549	76,354
						1,3	1,45	0,00414	0,004188	78,308	79,205
						1,4	1,818	0,005193	0,00523	81,079	81,995
						1,5	3,69795	0,010566	0,01049542	95,57886	95,092628
						2	4,179	0,01202	0,0119	99,754	98,306
				450	0,0045		0	0	0	49,068	48,896
						1	0,163	0,000465	0,000452	50,505	50,225
						1,1	0,325	0,00093	0,0009139	51,924	51,5269
						1,2	0,489	0,001396	0,001376	53,326	52,801
						1,3	0,652	0,00186	0,00184	54,713	54,05
						1,4	0,816	0,00233	0,002302	56,085	55,276
						1,5	1,63799	0,00468	0,00470772	62,77168	62,359107
						2	2,46834	0,007052	0,00709478	69,25739	69,604591
						2,5	3,30783	0,009451	0,00949772	75,6527	76,461917
						3	4,15816	0,01188	0,01191614	82,06806	82,970429
						3,5	5,02191	0,014348	0,01434953	88,63555	89,163019
						4	5,90342	0,016867	0,01679716	95,54742	95,067338
					0,00875	4,5	6,41	0,018497	0,01835	100,245	98,666
							0	0	0	63,05316	62,678609

			1	0,31132	0,000889	0,00092431	65,50608	65,443868
			1,1	0,62382	0,001782	0,0018224	67,93743	68,150883
			1,2	0,93757	0,002679	0,00272276	70,35291	70,801887
			1,3	1,25264	0,003579	0,00362535	72,75819	73,399135
			1,4	1,56911	0,004483	0,00453016	75,15894	75,944737
			1,5	3,17661	0,009076	0,00908636	87,3183	87,963219
		0,013		0	0	0	75,948	76,77
			1	0,465	0,00133	0,00137	79,454	80,369
			1,1	0,933	0,002666	0,002699	82,9887	83,869
			1,2	1,406	0,00402	0,00403	86,574	87,276
			1,3	1,883	0,00538	0,00537	90,24	90,594
			1,4	2,366	0,00676	0,00671	94,026	93,827
			1,5	3,03	0,008698	0,00857	99,549	98,156
	550	0,0045		0	0	0	52,514	52,065
			1	0,197	0,000564	0,000541	54,198	53,588
			1,1	0,395	0,001128	0,0011	55,861	55,076
			1,2	0,593	0,00169	0,00166	57,505	56,531
			1,3	0,792	0,00226	0,00227	59,131	59,122
			1,4	0,99	0,00283	0,00285	60,741	60,045
			1,5	1,99193	0,005691	0,00573263	68,62056	68,904948
			2	3,00661	0,00859	0,00863681	76,35199	77,191031
			2,5	4,0375	0,011536	0,01156341	84,13289	84,972634
			3	5,08976	0,014542	0,01451164	92,2159	92,306377
		0,00875	3,5	6,01	0,01733	0,01719	100,127	98,58
				0	0	0	69,03201	69,357211
			1	0,38076	0,001088	0,00113365	71,94899	72,530363
			1,1	0,76354	0,002182	0,00222854	74,85653	75,626794
			1,2	1,1485	0,003281	0,00332664	77,765	78,650051
			1,3	1,53584	0,004388	0,0044279	80,6855	81,603439
			1,4	1,92582	0,005502	0,00553226	83,63037	84,490027
			1,5	3,92944	0,011227	0,01109903	99,35856	98,014456
		0,013		0	0	0	84,535	85,357
			1	0,574	0,00164	0,001639	88,916	89,415
			1,1	1,557	0,0033	0,00326	93,448	93,347
			1,2	1,747	0,00499	0,00488	98,222	97,161
			1,3	N/A	N/A	N/A	N/A	N/A
40	350	0,0045		0	0	0	41,32033	41,566691
			1	0,12938	0,00037	0,00035606	42,36969	42,575547
			1,1	0,25889	0,00074	0,00069965	43,4051	43,565845
			1,2	0,38853	0,00111	0,00107369	44,4274	44,538077
			1,3	0,5183	0,001481	0,00144818	45,4374	45,493096
			1,4	0,6482	0,001852	0,00182311	46,43581	46,431686
			1,5	1,29983	0,003714	0,00370435	51,27649	50,901946
			2	1,95521	0,005586	0,00559661	55,91337	55,051745
			2,5	2,61468	0,007471	0,00749881	60,39998	59,565332
			3	3,27859	0,009367	0,00941152	64,77964	64,610374
			3,5	3,94736	0,011278	0,01133417	69,08995	69,459178
			4	4,62151	0,013204	0,01326651	73,3661	74,126674
			4,5	5,3017	0,015148	0,01520829	77,64375	78,626016
			5	5,98879	0,017111	0,01715954	81,96226	82,969487
			5,5	6,68399	0,019097	0,01911921	86,36914	87,165622
		0,00875		0	0	0	51,28902	50,913339
			1	0,24394	0,000697	0,0006728	53,03863	52,494696
			1,1	0,48843	0,001396	0,00136491	54,76305	54,034812
			1,2	0,73347	0,002096	0,00205782	56,46498	55,536313

		1,3	0,97908	0,002797	0,00281668	58,14691	56,934059
		1,4	1,22528	0,003501	0,00352683	59,81112	58,879769
		1,5	2,46588	0,007045	0,00709866	67,93838	68,176744
		2	3,72474	0,010642	0,01070446	75,9141	76,828945
		2,5	5,00648	0,014304	0,0143424	83,97859	84,919973
		3	6,3194	0,018055	0,01801139	92,45754	92,51817
	0,013		0	0	0	60,32266	59,475533
		1	0,36024	0,001029	0,00106632	62,71487	62,244965
		1,1	0,72186	0,002062	0,00210758	65,08153	64,95418
		1,2	1,08492	0,0031	0,00315177	67,42847	67,605785
		1,3	1,4495	0,004141	0,00419885	69,76135	70,202221
		1,4	1,8157	0,005188	0,00524877	72,08573	72,745765
		1,5	3,67513	0,0105	0,01053973	83,79006	84,739881
		2	5,3355	0,009139	0,009109	91,4966	91,789
450	0,0045		0	0	0	44,46827	44,57772
		1	0,16388	0,000468	0,00046284	45,74098	45,77905
		1,1	0,32798	0,000937	0,00092931	46,99556	46,95546
		1,2	0,49229	0,001407	0,00139612	48,23334	48,107453
		1,3	0,65684	0,001877	0,00186328	49,45555	49,236321
		1,4	0,82161	0,002347	0,0023308	50,66329	50,343248
		1,5	1,64915	0,004712	0,00467382	56,51922	55,583888
		2	2,48326	0,007095	0,00713003	62,1448	61,587651
		2,5	3,32472	0,009499	0,00955166	67,62405	67,824834
		3	4,17447	0,011927	0,01198896	73,02979	73,7653
		3,5	5,03376	0,014382	0,01444135	78,43357	79,435998
	0,00875		0	0	0	56,68652	55,730281
		1	0,31211	0,000892	0,00091391	58,8163	57,718313
		1,1	0,62519	0,001786	0,00181663	60,91891	60,168428
		1,2	0,93928	0,002684	0,00272174	62,99866	62,571549
		1,3	1,25441	0,003584	0,00362911	65,05956	64,929192
		1,4	1,57065	0,004488	0,0045387	67,10545	67,243086
		1,5	3,17029	0,009058	0,00911907	77,24052	78,20981
		2	4,80882	0,013739	0,01375125	87,59923	88,290736
	0,013		0	0	0	67,7663	67,984881
		1	0,46375	0,001325	0,00138417	70,72658	71,263967
		1,1	0,93018	0,002658	0,00272003	73,67693	74,459702
		1,2	1,39951	0,003999	0,00406039	76,6292	77,575712
		1,3	1,87201	0,005349	0,00540516	79,59611	80,615869
		1,4	2,34803	0,006709	0,00675426	82,59193	83,583747
550	0,0045		0	0	0	47,49317	47,419648
		1	0,19851	0,000567	0,00055497	48,97788	48,796136
		1,1	0,39736	0,001135	0,00111927	50,44088	50,140032
		1,2	0,59655	0,001704	0,00168409	51,88405	51,45324
		1,3	0,79609	0,002275	0,00224944	53,30911	52,737531
		1,4	0,996	0,002846	0,00281531	54,71763	53,99451
		1,5	2,00129	0,005718	0,00575078	61,56026	60,911859
		2	3,01717	0,00862	0,00867439	68,17708	68,443456
		2,5	4,04529	0,011558	0,01162053	74,69722	75,546038
		3	5,08807	0,014537	0,01458856	81,24925	82,266659
		3,5	6,14929	0,017569	0,01757753	87,99017	88,643729
		4	7,23567	0,020673	0,02058665	95,16041	94,710002
550	0,00875		0	0	0	61,85221	61,249611
		1	0,38098	0,001089	0,00113129	64,3572	64,128548
		1,1	0,76355	0,002182	0,00223197	66,83827	66,942517
		1,2	1,14779	0,003279	0,00333587	69,30212	69,694423

			1,3	1,5338	0,004382	0,00444295	71,75529	72,386979
			1,4	1,92171	0,005491	0,00555317	74,20442	75,022712
			1,5	3,89544	0,01113	0,01114961	86,65206	87,426148
		0,013		0	0	0	74,98245	75,848228
			1	0,56977	0,001628	0,0016869	78,56161	79,566757
			1,1	1,14452	0,00327	0,00331755	82,17558	83,177739
			1,2	1,72495	0,004928	0,00495445	85,85281	86,687141
			1,3	2,31208	0,006606	0,00659748	89,62939	90,100411
			1,4	2,90734	0,008307	0,00824651	93,55472	93,422536
50	350	0,0045		0	0	0	38,16494	38,522633
			1	0,1304	0,000373	0,00037541	39,11945	39,453378
			1,1	0,26091	0,000745	0,00074742	40,06047	40,366985
			1,2	0,39154	0,001119	0,00111963	40,98881	41,263784
			1,3	0,52229	0,001492	0,00149205	41,9052	42,144582
			1,4	0,65316	0,001866	0,00186467	42,81033	43,010125
			1,5	1,30936	0,003741	0,00373093	47,18761	47,131471
			2	1,96888	0,005625	0,00560258	51,36185	50,95663
			2,5	2,63195	0,00752	0,00747969	55,38078	54,536043
			3	3,2988	0,009425	0,00945575	59,28154	58,183194
			3,5	3,96973	0,011342	0,0113903	63,09476	62,650511
			4	4,64503	0,013272	0,01333449	66,84707	66,960299
			4,5	5,3251	0,015215	0,01528804	70,5631	71,123547
			5	6,01039	0,017173	0,01725072	74,26705	75,150127
			5,5	6,70151	0,019147	0,01922232	77,98432	79,048862
			6	7,39924	0,021141	0,02120263	81,74349	82,827678
		0,00875		0	0	0	47,137	47,084447
			1	0,24483	0,0007	0,0006853	48,7109	48,539572
			1,1	0,49012	0,0014	0,00138136	50,25946	49,956743
			1,2	0,7359	0,002103	0,00207818	51,78506	51,338409
			1,3	0,98217	0,002806	0,00277576	53,28988	52,686821
			1,4	1,22895	0,003511	0,00347408	54,77588	54,004004
			1,5	2,47089	0,00706	0,00710301	61,98348	61,356826
			2	3,72768	0,010651	0,01072006	68,95273	69,333503
			2,5	5,00187	0,014291	0,01436887	75,84407	76,822312
				6,29741	0,017993	0,01804841	82,82461	83,881045
		0,013		0	0	0	55,20924	54,385084
			1	0,36068	0,001031	0,00097969	57,33759	56,240152
			1,1	0,72251	0,002064	0,00209566	59,43601	58,36558
			1,2	1,08554	0,003102	0,0031427	61,50913	60,802397
			1,3	1,44981	0,004142	0,00419258	63,56126	63,191494
			1,4	1,81538	0,005187	0,00524527	65,59646	65,534777
			1,5	3,66501	0,010471	0,01054947	75,65423	76,622574
			2	5,56017	0,015886	0,01591868	85,90082	86,791861
	450	0,0045		0	0	0	41,00438	41,279062
			1	0,16488	0,000471	0,00047053	42,15774	42,386499
			1,1	0,32995	0,000943	0,00094047	43,29347	43,470287
			1,2	0,49522	0,001415	0,00141075	44,4128	44,531469
			1,3	0,66069	0,001888	0,00188136	45,51685	45,571264
			1,4	0,82636	0,002361	0,00235232	46,60665	46,590785
			1,5	1,65793	0,004737	0,00471225	51,87259	51,417269
			2	2,49519	0,007129	0,00708085	56,89899	55,860524
			2,5	3,33864	0,009539	0,00958127	61,75687	61,092112
			3	4,18888	0,011968	0,01202994	66,50327	66,569463
			3,5	5,04662	0,014419	0,01449362	71,18842	71,812402
			4	5,91284	0,016894	0,01697176	75,86107	76,840448

						4,5	6,78883	0,019397	0,01946394	80,57391	81,670745
						5	7,67644	0,021933	0,02196973	85,3906	86,318304
					0,00875		0	0	0	51,96793	51,503411
						1	0,31279	0,000894	0,00086065	53,8719	53,204389
						1,1	0,62639	0,00179	0,00174763	55,74673	54,856649
						1,2	0,94085	0,002688	0,00271048	57,596	56,186257
						1,3	1,25619	0,003589	0,0036204	59,42301	58,350235
						1,4	1,57243	0,004493	0,00453254	61,23079	60,476507
						1,5	3,16849	0,009053	0,00912518	70,07726	70,585786
						2	4,79355	0,013696	0,01376899	78,84069	79,924895
							6,45725	0,018449	0,01846079	87,89266	88,6034
					0,013		0	0	0	61,80347	61,146572
						1	0,46336	0,001324	0,00137766	64,40491	64,166192
						1,1	0,92886	0,002654	0,00271734	66,98164	67,113063
						1,2	1,39662	0,00399	0,00406145	69,54161	69,99069
						1,3	1,86679	0,005334	0,00540992	72,09265	72,802333
						1,4	2,33954	0,006684	0,00676267	74,64277	75,55101
				550	0,0045		0	0	0	43,7276	43,882713
						1	0,19948	0,00057	0,00056451	45,06865	45,149965
						1,1	0,39925	0,001141	0,00113248	46,38837	46,387118
						1,2	0,59932	0,001712	0,00170095	47,68846	47,595961
						1,3	0,7997	0,002285	0,00226992	48,97045	48,778154
						1,4	1,0004	0,002858	0,00283939	50,23577	49,935199
						1,5	2,00885	0,00574	0,00569433	56,35432	55,387149
						2	3,02624	0,008646	0,00869078	62,2167	61,62895
						2,5	4,0536	0,011582	0,01164811	67,92385	68,178077
						3	5,09228	0,014549	0,01462711	73,5632	74,395149
						3,5	6,14419	0,017555	0,01762682	79,22249	80,312507
						4	7,21219	0,020606	0,02064652	85,00501	85,957911
					0,00875		0	0	0	56,5691	55,574739
						1	0,3813	0,001089	0,00111767	58,79284	57,605493
						1,1	0,76391	0,002183	0,00222133	60,98688	60,190579
						1,2	1,14789	0,00328	0,00332821	63,15636	62,722099
						1,3	1,5333	0,004381	0,00443822	65,30613	65,202223
						1,4	1,92022	0,005486	0,00555133	67,44081	67,63307
						1,5	3,88033	0,011087	0,01116161	78,04687	79,113001
						2	5,89589	0,016845	0,01684316	89,02993	89,611356
					0,013		0	0	0	68,12668	68,406737
						1	0,56778	0,001622	0,00169702	71,21838	71,845419
						1,1	1,13925	0,003255	0,00333321	74,3047	75,190376
						1,2	1,71477	0,004899	0,0049756	77,40039	78,446636
						1,3	2,29478	0,006557	0,00662405	80,52177	81,618817
						1,4	2,87984	0,008228	0,00827845	83,68771	84,711159
Carbon	1	0	30	350	0,0045	1	0	0	0	45,99558	46,459499
						1,1	0,01654	4,73E-05	4,7145E-05	47,85258	48,235328
						1,2	0,03313	9,47E-05	9,4353E-05	49,66217	49,948443
						1,3	0,04976	0,000142	0,00014165	51,42946	51,60374
						1,4	0,06643	0,00019	0,00018903	53,15888	53,206171
						1,5	0,08315	0,000238	0,00023649	54,85429	54,760017
						2	0,16742	0,000478	0,00047497	62,9284	61,916384
						2,5	0,25289	0,000723	0,00072712	70,54277	69,4638
						3	0,3397	0,000971	0,00097762	77,91758	78,297461
						3,5	0,42806	0,001223	0,00123127	85,24109	86,550119
						4	0,51837	0,001481	0,00148789	92,72147	94,293558
						4,5	0,61134	0,001747	0,00174731	100,6662	101,58523

		0,00875	1	0	0	0	63,48971	62,398236
			1,1	0,03228	9,22E-05	8,7336E-05	66,40544	64,867492
			1,2	0,06474	0,000185	0,00018904	69,2711	67,898872
			1,3	0,09738	0,000278	0,00028338	72,09791	71,362593
			1,4	0,13022	0,000372	0,0003782	74,8963	74,733308
			1,5	0,16327	0,000466	0,00047348	77,67629	78,015915
			2	0,33222	0,000949	0,00095646	91,6701	93,252648
			2,5	0,51091	0,00146	0,00144961	107,3522	106,83362
		0,013	1	0	0	0	78,53446	79,014641
			1,1	0,04864	0,000139	0,00014701	82,57147	83,611246
			1,2	0,09782	0,000279	0,00028771	86,63039	88,045492
			1,3	0,14761	0,000422	0,00042931	90,74946	92,328268
			1,4	0,19814	0,000566	0,00057177	94,97691	96,469335
			1,5	0,24956	0,000713	0,00071507	99,37958	100,47747
	450	0,0045	1	0	0	0	51,71657	51,871087
			1,1	0,02126	6,07E-05	5,9815E-05	53,90603	53,892905
			1,2	0,04258	0,000122	0,00012033	56,04278	55,838885
			1,3	0,06398	0,000183	0,00018097	58,13338	57,715911
			1,4	0,08546	0,000244	0,00024175	60,18356	59,530089
			1,5	0,10701	0,000306	0,00030264	62,19835	61,286676
			2	0,21595	0,000617	0,00062208	71,8857	71,10451
			2,5	0,32712	0,000935	0,00094246	81,23904	82,113445
			3	0,44108	0,00126	0,00126781	90,65674	92,234478
			3,5	0,55901	0,001597	0,00159777	100,6809	101,59754
		0,00875	1	0	0	0	72,50119	71,852158
			1,1	0,0418	0,000119	0,00012594	76,04923	76,103117
			1,2	0,08394	0,00024	0,00024731	79,57422	80,214955
			1,3	0,12646	0,000361	0,00036941	83,09695	84,196439
			1,4	0,16939	0,000484	0,0004922	86,63977	88,05551
			1,5	0,21279	0,000608	0,00061568	90,22828	91,799352
			2	0,44104	0,00126	0,00124262	110,526	108,99906
		0,013	1	0	0	0	91,08635	92,668258
			1,1	0,06406	0,000183	0,00018767	96,46841	97,863565
			1,2	0,12968	0,000371	0,00036921	102,1817	102,85133
			1,3	0,19762	0,000565	0,00055203	108,5059	107,64661
	550	0,0045	1	0	0	0	57,01783	56,71832
			1,1	0,02601	7,43E-05	7,2081E-05	59,52484	58,949972
			1,2	0,05212	0,000149	0,00014591	61,97745	61,095275
			1,3	0,07836	0,000224	0,00021991	64,38389	63,16183
			1,4	0,1047	0,000299	0,00029409	66,75143	65,156769
			1,5	0,13117	0,000375	0,00037877	69,08664	67,671018
			2	0,26547	0,000758	0,00076615	80,48002	81,251223
			2,5	0,40381	0,001154	0,0011609	91,92353	93,505323
			3	0,54849	0,001567	0,00156238	104,4506	104,66496
		0,00875	1	0	0	0	81,08043	81,934013
			1,1	0,05163	0,000148	0,00015578	85,34688	86,665074
			1,2	0,10392	0,000297	0,00030476	89,66595	91,224321
			1,3	0,15699	0,000449	0,00045471	94,09011	95,623394
			1,4	0,211	0,000603	0,0006056	98,69146	99,872825
			1,5	0,26626	0,000761	0,00075741	103,5815	103,98207
		0,013	1	N/A	N/A	N/A	N/A	N/A
40	350	0,0045	1	0	0	0	40,2071	40,821526
			1,1	0,01654	4,73E-05	4,7531E-05	41,79865	42,391989
			1,2	0,03311	9,46E-05	9,4812E-05	43,34655	43,907163
			1,3	0,04972	0,000142	0,00014217	44,85523	45,3718

		1,4	0,06637	0,00019	0,0001896	46,32851	46,790242
		1,5	0,08305	0,000237	0,00023711	47,76965	48,166244
		2	0,16698	0,000477	0,00047569	54,58348	54,511099
		2,5	0,25181	0,000719	0,00071595	60,91529	60,155259
		3	0,33758	0,000965	0,00096877	66,92882	64,931485
		3,5	0,42437	0,001212	0,00121967	72,74026	72,124149
		4	0,51226	0,001464	0,00147321	78,44417	78,923479
		4,5	0,60143	0,001718	0,00172931	84,12952	85,371961
		5	0,69209	0,001977	0,00198783	89,8944	91,503417
	0,00875	1	0	0	0	55,09069	54,973327
		1,1	0,03214	9,18E-05	8,9601E-05	57,52936	57,168422
		1,2	0,06441	0,000184	0,00018095	59,91118	59,277092
		1,3	0,09682	0,000277	0,00027252	62,24436	61,307035
		1,4	0,12936	0,00037	0,00036431	64,53608	63,265538
		1,5	0,16205	0,000463	0,0004672	66,79271	64,761119
		2	0,32776	0,000936	0,00094581	77,74011	78,100384
		2,5	0,49802	0,001423	0,00143368	88,58572	90,151217
		3	0,67488	0,001928	0,00192998	100,1096	101,13817
	0,013	1	0	0	0	67,57654	65,744198
		1,1	0,04811	0,000137	0,00014369	70,81088	69,761606
		1,2	0,09655	0,000276	0,00028363	74,00291	73,653887
		1,3	0,14534	0,000415	0,00042438	77,16788	77,428354
		1,4	0,1945	0,000556	0,00056592	80,32082	81,092003
		1,5	0,24408	0,000697	0,00070823	83,47722	84,65117
		2	0,50008	0,001429	0,00143065	100,0243	101,06472
450	0,0045	1	0	0	0	45,10365	45,612915
		1,1	0,02123	6,06E-05	6,0559E-05	46,96845	47,402552
		1,2	0,04251	0,000121	0,00012116	48,7832	49,126931
		1,3	0,06385	0,000182	0,00018187	50,55341	50,791053
		1,4	0,08525	0,000244	0,0002427	52,28386	52,400271
		1,5	0,1067	0,000305	0,00030364	53,97866	53,95919
		2	0,21487	0,000614	0,00060989	62,03114	61,122782
		2,5	0,32458	0,000927	0,00093301	69,60185	68,267876
		3	0,43601	0,001246	0,00125479	76,91597	77,131334
		3,5	0,54943	0,00157	0,00158073	84,16108	85,406507
		4	0,66529	0,001901	0,00191062	91,53877	93,167103
	0,00875	1	0	0	0	62,61833	61,628875
		1,1	0,04148	0,000119	0,00011262	65,52155	64,096523
		1,2	0,08319	0,000238	0,00024269	68,37208	66,738343
		1,3	0,12514	0,000358	0,00036397	71,18135	70,217352
		1,4	0,16735	0,000478	0,00048589	73,9599	73,602009
		1,5	0,20982	0,000599	0,00060843	76,71779	76,897227
		2	0,42689	0,00122	0,00122986	90,56028	92,181661
	0,013	1	0	0	0	77,57562	77,908023
		1,1	0,06252	0,000179	0,00018916	81,57615	82,521159
		1,2	0,12573	0,000359	0,00037025	85,59283	86,970057
		1,3	0,18971	0,000542	0,00055252	89,66253	91,2657
		1,4	0,25461	0,000727	0,00073595	93,83107	95,418111
		1,5	0,32064	0,000916	0,00092049	98,16088	99,436287
550	0,0045	1	0	0	0	49,6178	49,913895
		1,1	0,02594	7,41E-05	7,335E-05	51,73795	51,894377
		1,2	0,05197	0,000148	0,00014728	53,80373	53,798982
		1,3	0,07808	0,000223	0,00022137	55,82175	55,634766
		1,4	0,10428	0,000298	0,00029562	57,79775	57,40798
		1,5	0,13056	0,000373	0,00037002	59,73671	59,123981

			2	0,26336	0,000752	0,00075779	69,01611	67,540392
			2,5	0,39867	0,001139	0,00114846	77,89212	78,278794
			3	0,53698	0,001534	0,00154525	86,7047	88,165918
			3,5	0,67929	0,001941	0,00194768	95,84467	97,325718
		0,00875	1	0	0	0	69,64369	68,319571
			1,1	0,05098	0,000146	0,00015297	73,02401	72,468773
			1,2	0,10234	0,000292	0,0003012	76,36907	76,484376
			1,3	0,15411	0,00044	0,00045032	79,6965	80,374768
			1,4	0,20632	0,000589	0,0006003	83,02428	84,147553
			1,5	0,25904	0,00074	0,00075112	86,37184	87,809606
		0,013	1	0	0	0	87,24046	88,736338
			1,1	0,07771	0,000222	0,0002315	92,20271	93,827574
			1,2	0,15693	0,000448	0,00045368	97,36177	98,718718
			1,3	0,23815	0,00068	0,00067745	102,8661	103,42433
50	350	0,0045	1	0	0	0	36,19114	36,814264
			1,1	0,01654	4,73E-05	4,7692E-05	37,60566	38,237882
			1,2	0,03311	9,46E-05	9,5014E-05	38,97986	39,612446
			1,3	0,04971	0,000142	0,00014241	40,3177	40,941545
			1,4	0,06634	0,00019	0,00018987	41,62261	42,229092
			1,5	0,083	0,000237	0,0002374	42,89751	43,47847
			2	0,16674	0,000476	0,00047599	48,90208	49,244174
			2,5	0,25123	0,000718	0,00071613	54,44044	54,380199
			3	0,33647	0,000961	0,00095765	59,65276	59,042326
			3,5	0,42249	0,001207	0,00120047	64,63311	63,331688
			4	0,50933	0,001455	0,0014622	69,45107	68,055583
			4,5	0,59705	0,001706	0,00171567	74,16299	73,841062
			5	0,68572	0,001959	0,00197138	78,819	79,369348
			5,5	0,77546	0,002216	0,00222921	83,46839	84,662202
		0,00875	1	0	0	0	49,36467	49,680464
			1,1	0,03207	9,16E-05	9,0709E-05	51,504	51,679594
			1,2	0,06424	0,000184	0,00018212	53,58702	53,600561
			1,3	0,09653	0,000276	0,00027373	55,62072	55,450686
			1,4	0,12892	0,000368	0,00036555	57,6111	57,23654
			1,5	0,16142	0,000461	0,00045755	59,56336	58,963733
			2	0,32568	0,000931	0,0009371	68,89875	67,366522
			2,5	0,49309	0,001409	0,00142055	77,82318	78,204819
			3	0,66429	0,001898	0,00191176	86,68747	88,173325
		0,013	1	0	0	0	60,28065	59,592366
			1,1	0,04786	0,000137	0,00013113	63,06367	61,997747
			1,2	0,09597	0,000274	0,00026667	65,7903	64,303877
			1,3	0,14433	0,000412	0,0004187	68,47119	66,831937
			1,4	0,19296	0,000551	0,00055932	71,11596	70,118965
			1,5	0,24188	0,000691	0,00070064	73,7335	73,321145
			2	0,49123	0,001404	0,00141728	86,71239	88,199511
	450	0,0045	1	0	0	0	40,53911	41,160766
			1,1	0,02121	6,06E-05	6,09E-05	42,19065	42,786693
			1,2	0,04247	0,000121	0,00012154	43,79533	44,353047
			1,3	0,06378	0,000182	0,00018228	45,35809	45,865197
			1,4	0,08514	0,000243	0,00024313	46,88315	47,327965
			1,5	0,10654	0,000304	0,00030408	48,37413	48,745501
			2	0,21429	0,000612	0,00061025	55,41655	55,265849
			2,5	0,32327	0,000924	0,00091871	61,95803	61,048446
			3	0,43355	0,001239	0,00124484	68,17638	66,462665
			3,5	0,54522	0,001558	0,00156765	74,19868	73,885078
			4	0,65845	0,001881	0,00189398	80,13064	80,887103

50	G	1	0	30	450	0,0045	2	0,0046238	0,00474002	-2,512
51	G	0,75	0	30	450	0,00875	1,5	0,0046604	0,00452763	2,849
52	G	0,75	0,01	40	550	0,013	1,3	0,0049284	0,0048157	2,287
53	G	1	0	50	350	0,013	1,5	0,0051946	0,00523193	-0,718
54	G	0,5	0,002	40	350	0,013	1,5	0,005255	0,00523193	0,439
55	G	0,5	0,002	50	450	0,013	1,4	0,00539	0,00533345	1,049
56	G	1	0,01	40	550	0,0045	2	0,005718	0,00579336	-1,318
57	G	0,75	0,01	40	550	0,013	1,4	0,0066059	0,00651866	1,321
58	G	0,5	0,01	30	350	0,00875	2	0,0070299	0,00716855	-1,972
59	G	1	0	30	450	0,0045	2,5	0,007032	0,00715154	-1,699
60	G	0,75	0,002	40	350	0,00875	2	0,0070364	0,00716855	-1,878
61	G	0,5	0,01	30	350	0,0045	3	0,0074079	0,00743794	-0,405
62	G	0,75	0,01	40	550	0,013	1,5	0,0083067	0,00822161	1,024
63	G	1	0,01	40	550	0,0045	2,5	0,0086205	0,00874077	-1,396
64	G	0,75	0	40	450	0,0045	3	0,0093174	0,00956306	-2,637
65	G	0,5	0	30	450	0,0045	3	0,009552	0,00956306	-0,116
66	G	0,5	0,01	30	350	0,00875	2,5	0,0106412	0,0108156	-1,639
67	G	0,75	0,002	40	350	0,00875	2,5	0,0107083	0,0108156	-1,002
68	G	0,75	0	50	350	0,0045	4	0,0107926	0,01118919	-3,674
69	G	0,75	0	40	550	0,0045	3	0,0115564	0,01168819	-1,141
70	G	1	0,002	30	450	0,0045	3,5	0,0120781	0,01197458	0,857

Appendix B

Below is a list of detailed input value and results of the 70 examples solved for flat laminates and presented in Fig 27.

Nr	FRP	B/H	ρ_s'	f_c'	f_y	ρ_s	$\overline{M_n}/M_n$	ρ_f (exact)	ρ_f (lin. reg) linear reg.	% difference
1	C	0,5	0	40	550	0,0045	1,2	0,0001488	0,00014367	3,424
2	C	0,5	0	40	550	0,0045	1,3	0,0002237	0,00022226	0,659
3	C	1	0,01	40	550	0,00875	1,2	0,00029	0,00027935	3,672
4	C	1	0,002	30	550	0,00875	1,2	0,0002969	0,00027935	5,919
5	C	0,5	0	40	550	0,0045	1,4	0,0002991	0,00030086	-0,579
6	C	0,5	0,002	50	350	0,013	1,3	0,0004124	0,00040861	0,915
7	C	0,75	0,002	30	350	0,013	1,3	0,0004217	0,00040861	3,117
8	C	1	0	30	350	0,013	1,3	0,0004279	0,00040861	4,500
9	C	1	0,01	40	550	0,00875	1,3	0,0004359	0,00043218	0,857
10	C	1	0	30	350	0,00875	1,5	0,0004686	0,00046953	-0,195
11	C	0,5	0,002	50	350	0,013	1,4	0,0005513	0,0005531	-0,321
12	C	1	0	30	350	0,013	1,4	0,0005764	0,0005531	4,045
13	C	1	0,01	40	550	0,00875	1,4	0,0005825	0,00058501	-0,433
14	C	0,5	0,002	50	350	0,013	1,5	0,0006911	0,00069759	-0,943
15	C	1	0,01	30	450	0,013	1,4	0,0007144	0,00071113	0,459
16	C	0,75	0,002	50	550	0,00875	1,5	0,0007324	0,00073784	-0,739
17	C	0,75	0,01	50	350	0,0045	2,5	0,0007417	0,00074164	0,002
18	C	0,5	0,01	50	550	0,013	1,4	0,0008713	0,00086915	0,245
19	G	0,75	0,002	30	450	0,0045	1,2	0,0009142	0,00088158	3,572
20	C	1	0	30	350	0,00875	2	0,0009594	0,00095581	0,378
21	C	0,75	0,01	50	350	0,0045	3	0,0009915	0,00099173	-0,019
22	C	0,75	0,01	50	350	0,0045	3,5	0,0012429	0,00124181	0,085
23	C	0,5	0,002	50	350	0,013	2	0,0014035	0,00142006	-1,178
24	C	0,5	0,01	30	350	0,0045	4	0,0014805	0,00149189	-0,772
25	C	0,75	0,002	50	550	0,00875	2	0,0014901	0,00150198	-0,800
26	G	0,5	0	50	550	0,0045	1,3	0,0016582	0,00166697	-0,531
27	C	1	0,002	40	350	0,0045	4,5	0,0017184	0,00174198	-1,374
28	C	0,5	0,01	30	350	0,0045	4,5	0,0017346	0,00174198	-0,423
29	C	0,5	0	30	350	0,0045	4,5	0,0017623	0,00174198	1,152
30	G	0,5	0,002	40	350	0,0045	1,5	0,001785	0,00181105	-1,460
31	G	1	0,002	30	450	0,00875	1,2	0,0018036	0,00171419	4,959
32	G	0,5	0,002	30	450	0,0045	1,4	0,001835	0,00184619	-0,610
33	C	1	0,01	50	450	0,0045	4	0,0019028	0,00191815	-0,809
34	C	1	0,002	40	350	0,0045	5	0,0019774	0,00199206	-0,741
35	C	0,75	0,002	30	350	0,0045	5	0,0020249	0,00199206	1,620
36	C	1	0,01	50	450	0,0045	4,5	0,0022312	0,00223968	-0,382
37	C	1	0,002	40	350	0,0045	5,5	0,0022418	0,00224214	-0,014
38	G	1	0,01	40	550	0,0045	1,4	0,0022746	0,00225646	0,796
39	G	0,5	0	30	450	0,0045	1,5	0,0022849	0,0023285	-1,906
40	C	0,75	0,01	40	450	0,00875	3	0,0024619	0,00247931	-0,709
41	C	0,5	0,01	550	450	0,0045	5	0,0025635	0,00256122	0,090
42	G	1	0,002	30	450	0,00875	1,3	0,0027188	0,002652	2,457
43	G	1	0,01	40	550	0,0045	1,5	0,0028457	0,00284594	-0,008
44	G	1	0,002	30	350	0,013	1,3	0,0031832	0,00306454	3,729
45	G	0,5	0	30	350	0,013	1,3	0,003248	0,00306454	5,648
46	G	0,75	0,01	40	550	0,013	1,2	0,00327	0,00311275	4,810
47	G	0,75	0,002	40	350	0,00875	1,5	0,003477	0,00352149	-1,281
48	G	0,5	0,01	30	350	0,00875	1,5	0,003488	0,00352149	-0,961
49	G	1	0	50	350	0,013	1,4	0,0041414	0,00414824	-0,166

50	G	1	0	30	450	0,0045	2	0,0046238	0,00474002	-2,512
51	G	0,75	0	30	450	0,00875	1,5	0,0046604	0,00452763	2,849
52	G	0,75	0,01	40	550	0,013	1,3	0,0049284	0,0048157	2,287
53	G	1	0	50	350	0,013	1,5	0,0051946	0,00523193	-0,718
54	G	0,5	0,002	40	350	0,013	1,5	0,005255	0,00523193	0,439
55	G	0,5	0,002	50	450	0,013	1,4	0,00539	0,00533345	1,049
56	G	1	0,01	40	550	0,0045	2	0,005718	0,00579336	-1,318
57	G	0,75	0,01	40	550	0,013	1,4	0,0066059	0,00651866	1,321
58	G	0,5	0,01	30	350	0,00875	2	0,0070299	0,00716855	-1,972
59	G	1	0	30	450	0,0045	2,5	0,007032	0,00715154	-1,699
60	G	0,75	0,002	40	350	0,00875	2	0,0070364	0,00716855	-1,878
61	G	0,5	0,01	30	350	0,0045	3	0,0074079	0,00743794	-0,405
62	G	0,75	0,01	40	550	0,013	1,5	0,0083067	0,00822161	1,024
63	G	1	0,01	40	550	0,0045	2,5	0,0086205	0,00874077	-1,396
64	G	0,75	0	40	450	0,0045	3	0,0093174	0,00956306	-2,637
65	G	0,5	0	30	450	0,0045	3	0,009552	0,00956306	-0,116
66	G	0,5	0,01	30	350	0,00875	2,5	0,0106412	0,0108156	-1,639
67	G	0,75	0,002	40	350	0,00875	2,5	0,0107083	0,0108156	-1,002
68	G	0,75	0	50	350	0,0045	4	0,0107926	0,01118919	-3,674
69	G	0,75	0	40	550	0,0045	3	0,0115564	0,01168819	-1,141
70	G	1	0,002	30	450	0,0045	3,5	0,0120781	0,01197458	0,857

Appendix C

Below is a sample of listing of the design variables used in the parametric study for wrapped laminates. This listing includes 217 data out of the 826 ones used for this paper. Due to space limitations, it was not possible to report all data sets.

FRP	***B/H***	$\rho' s$	η	f'_c	f_y	ρ_s	h_f	t_{fv}	t_{fh}	$\overline{M_n}/M_n$	ρ_f *(exact)*	ρ_f*(lin.Reg.)*
Glass	0,5	0,01	1,5	30	350	0,013	0	0	0	1	0	0
							20	2	3	1,91587	0,009714	0,0099151
							30	2	3	1,9602	0,010286	0,0103997
							60	1,8	2,7	1,97116	0,0108	0,0105195
						0,00875	0	0	0	1	0	0
							20	1	1,5	1,68962	0,004857	0,0050091
							30	2	3	2,43038	0,010286	0,0104588
							60	2,5	3,75	2,98422	0,015	0,0145334
						0,0045	0	0	0	1	0	0
							30	3	4,5	5,03169	0,015429	0,015221
							60	2	3	4,05662	0,012	0,0115318
							20	2	3	3,59307	0,009714	0,0097779
					450	0,013	0	0	0	1	0	0
							20	1	1,5	1,35925	0,004857	0,0049257
							30	1	1,5	1,37703	0,005143	0,0051757
							60	1	1,5	1,42311	0,006	0,0058232
						0,00875	0	0	0	1	0	0
							20	2	3	2,06087	0,009714	0,0099519
							30	2,5	3,75	2,3781	0,012857	0,0129525
							60	2	3	2,24566	0,012	0,0116998
						0,0045	0	0	0	1	0	0
							30	2	3	3,14171	0,010286	0,010376
							60	3	4,5	4,54083	0,018	0,0171821
							20	1	1,5	2,03065	0,004857	0,0049711
					550	0,013	0	0	0	1	0	0
							20	1	1,5	1,28997	0,004857	0,0048303
							30	1	1,5	1,30412	0,005143	0,0050735
							60	0,8	1,2	1,2742	0,0048	0,0045595
						0,00875	0	0	0	1	0	0
							20	1	1,5	1,43913	0,004857	0,0049757
							30	2	3	1,90618	0,010286	0,0103752
							60	1,8	2,7	1,91628	0,0108	0,0104919
						0,0045	0	0	0	1	0	0
							20	1	1,5	1,84919	0,004857	0,0049969
							30	1,5	2,25	2,33055	0,007714	0,0078589
							60	2,6	3,9	3,54355	0,0156	0,0150709
				40	350	0,013	0	0	0	1	0	0
							20	2	3	1,9206	0,009714	0,0099668
							30	2	3	1,96597	0,010286	0,0104627
							60	2,5	3,75	2,34205	0,015	0,0145734
						0,00875	0	0	0	1	0	0
							20	2	3	2,36259	0,009714	0,0099601
							30	3	4,5	3,12047	0,015429	0,0155357
							60	3	4,5	3,37293	0,018	0,0173931
						0,0045	0	0	0	1	0	0
							20	0,6	0,9	1,78056	0,002914	0,0029202
							30	4	6	6,29003	0,020571	0,019982
							60	2	3	4,03912	0,012	0,0114656

	450	0,013	0	0	0	1	0	0
			20	1	1,5	1,36119	0,004857	0,004953
			30	1	1,5	1,37926	0,005143	0,0052069
			60	1,5	2,25	1,63416	0,009	0,0087891
		0,00875	0	0	0	1	0	0
			20	2	3	2,06366	0,009714	0,0099783
			30	3	4,5	2,65225	0,015429	0,0155457
			60	2,5	3,75	2,55328	0,015	0,0146096
		0,0045	0	0	0	1	0	0
			20	1	1,5	2,02388	0,004857	0,0049382
			30	4	6	5,16825	0,020571	0,0202341
			60	3	4,5	4,54746	0,018	0,0172143
	550	0,013	0	0	0	1	0	0
			20	1	1,5	1,29366	0,004857	0,0048938
			30	1	1,5	1,30826	0,005143	0,0051445
			60	1,2	1,8	1,41369	0,0072	0,0069554
		0,00875	0	0	0	1	0	0
			20	2,8	4,2	2,20485	0,0136	0,013828
			30	2	3	1,91284	0,010286	0,0104521
			60	2	3	2,02357	0,012	0,0117323
		0,0045	0	0	0	1	0	0
			20	1	1,5	1,84509	0,004857	0,0049726
			30	1	1,5	1,88783	0,005143	0,0052267
			60	3,2	4,8	4,10807	0,0192	0,0117264
50	350	0,013	0	0	0	1	0	0
			20	1	1,5	1,46537	0,004857	0,004991
			30	1,5	2,25	1,73	0,007714	0,0078836
			60	2,5	3,75	2,35136	0,015	0,0146751
		0,00875	0	0	0	1	0	0
			20	1	1,5	1,68579	0,004857	0,004981
			30	2	3	2,42926	0,010286	0,0104506
			60	3,5	5,25	3,76052	0,021	0,0202445
		0,0045	0	0	0	1	0	0
			20	1	1,5	2,28814	0,004857	0,0048406
			30	2	3	3,68738	0,010286	0,0101347
			60	3	4,5	5,48975	0,018	0,0169541
	450	0,013	0	0	0	1	0	0
			20	1	1,5	1,36213	0,004857	0,0049663
			30	1	1,5	1,38035	0,005143	0,0052223
			60	2	3	1,84474	0,012	0,0117484
		0,00875	0	0	0	1	0	0
			20	0,6	0,9	1,32299	0,002914	0,0029725
			30	2	3	2,11776	0,010286	0,0104901
			60	3	4,5	2,86002	0,018	0,017511
		0,0045	0	0	0	1	0	0
			20	1	1,5	2,01859	0,004857	0,0049124
			30	2,6	3,9	3,74805	0,013371	0,0133255
			60	3,5	5,25	5,11301	0,021	0,0199654
	550	0,013	0	0	0	1	0	0
			20	1	1,5	1,29541	0,004857	0,0049238
			30	2	3	1,61268	0,010286	0,0103733
			60	1,8	2,7	1,6202	0,0108	0,0105024
		0,00875	0	0	0	1	0	0
			20	1	1,5	1,44018	0,004857	0,0049878
			30	3	4,5	2,35877	0,015429	0,0156075
			60	2	3	2,02893	0,012	0,0117942

						0,0045	0	0	0	1	0	0
							20	0,8	1,2	1,67438	0,003886	0,0039576
							30	1,8	2,7	2,58225	0,009257	0,0093554
							60	3,5	5,25	4,39486	0,021	0,0201324
Carbon	0,75	0,002	1	30	350	0,013	0	0	0	1	0	0
							20	0,3	0,3	1,6654	0,000971	0,000957
							30	0,3	0,3	1,6959	0,001029	0,0010014
							60	0,25	0,25	1,65411	0,001	0,0009405
						0,00875	0	0	0	1	0	0
							20	0,45	0,45	2,48716	0,001457	0,0014502
							30	0,4	0,4	2,39584	0,001371	0,0013606
							60	0,35	0,35	2,37335	0,0014	0,0013386
						0,0045	0	0	0	1	0	0
							30	0,6	0,6	4,99767	0,002057	0,0020123
							60	0,45	0,45	4,42562	0,0018	0,0017237
							20	0,6	0,6	4,82957	0,001943	0,0019275
					450	0,013	0	0	0	1,4907	0	0,0009031
							20	N/A	N/A	N/A	N/A	N/A
							30	N/A	N/A	N/A	N/A	N/A
							60	N/A	N/A	N/A	N/A	N/A
						0,00875	0	0	0	1	0	0
							20	0,35	0,35	1,90112	0,001133	0,0011254
							30	0,35	0,35	1,94239	0,0012	0,0011775
							60	0,3	0,3	1,90939	0,0012	0,0011359
						0,0045	0	0	0	1	0	0
							30	0,55	0,55	3,86471	0,001886	0,0018524
							60	0,45	0,45	3,65448	0,0018	0,001716
							20	0,4	0,4	3,03888	0,001295	0,0013168
					550	0,013	0	0	0	1	0	0
							20	N/A	N/A	1	N/A	N/A
							30	N/A	N/A	1	N/A	N/A
							60	N/A	N/A	1	N/A	N/A
						0,00875	0	0	0	1	0	0
							20	0,3	0,3	1,62396	0,000971	0,0009483
							30	0,25	0,25	1,5512	0,000857	0,0008362
							60	0,2	0,2	1,49819	0,0008	0,0007545
						0,0045	0	0	0	1	0	0
							20	0,5	0,5	3,0462	0,001619	0,0016152
							30	0,5	0,5	3,13778	0,001714	0,0016878
							60	0,43	0,43	3,07062	0,00172	0,0016345
				40	350	0,013	0	0	0	1	0	0
							20	0,46	0,46	2,03265	0,00149	0,0014922
							30	0,4	0,4	1,94789	0,001371	0,0013687
							60	0,36	0,36	1,95809	0,00144	0,0013836
						0,00875	0	0	0	1	0	0
							20	0,63	0,63	3,09242	0,00204	0,0020439
							30	0,59	0,59	3,06034	0,002023	0,0020124
							60	0,5	0,5	2,96901	0,002	0,0019229
						0,0045	0	0	0	1	0	0
							20	0,75	0,75	5,8125	0,002429	0,0024234
							30	0,7	0,7	5,72454	0,0024	0,002379
							60	0,63	0,63	5,773	0,00252	0,0024034
					450	0,013	0	0	0	1	0	0
							20	0,35	0,35	1,60816	0,001133	0,0011232
							30	0,3	0,3	1,55032	0,001029	0,0010148
							60	0,25	0,25	1,51684	0,001	0,0009521

		0,00875	0	0	0	1	0	0
			20	0,54	0,54	2,3972	0,001749	0,0017511
			30	0,5	0,5	2,36115	0,001714	0,0017056
			60	0,44	0,44	2,3466	0,00176	0,0016873
		0,0045	0	0	0	1	0	0
			20	0,74	0,74	4,69567	0,002396	0,0023914
			30	0,7	0,7	4,67293	0,0024	0,0023766
			60	0,6	0,6	4,54827	0,0024	0,0022958
	550	0,013	0	0	0	1	0	0
			20	N/A	N/A	1	N/A	N/A
			30	N/A	N/A	1	N/A	N/A
			60	N/A	N/A	1	N/A	N/A
		0,00875	0	0	0	1	0	0
			20	0,45	0,45	1,95277	0,001457	0,0014552
			30	0,4	0,4	1,89303	0,001371	0,0013631
			60	0,36	0,36	1,90233	0,00144	0,0013774
		0,0045	0	0	0	1	0	0
			20	0,69	0,69	3,82917	0,002234	0,0022359
			30	0,65	0,65	3,80104	0,002229	0,0022136
			60	0,55	0,55	3,67379	0,0022	0,0021127
50	350	0,013	0	0	0	1	0	0
			20	0,58	0,58	2,31298	0,001878	0,0019008
			30	0,5	0,5	2,19456	0,001714	0,0017282
			60	0,45	0,45	2,20851	0,0018	0,0017485
		0,00875	0	0	0	1	0	0
			20	0,74	0,74	3,47771	0,002396	0,0024219
			30	0,7	0,7	3,46257	0,0024	0,002407
			60	0,6	0,6	3,37892	0,0024	0,002325
		0,0045	0	0	0	1	0	0
			20	0,9	0,9	6,7863	0,002914	0,0029146
			30	0,85	0,85	6,74282	0,002914	0,0028927
			60	0,7	0,7	6,34765	0,0028	0,0026933
	450	0,013	0	0	0	1	0	0
			20	0,4	0,4	1,70806	0,001295	0,0013104
			30	0,4	0,4	1,74231	0,001371	0,0013745
			60	0,35	0,35	1,7309	0,0014	0,0013532
		0,00875	0	0	0	1	0	0
			20	0,65	0,65	2,69735	0,002105	0,0021296
			30	0,6	0,6	2,64842	0,002057	0,0020679
			60	0,45	0,45	2,40255	0,0018	0,0017578
		0,0045	0	0	0	1	0	0
			20	0,83	0,83	5,18116	0,002688	0,0027063
			30	0,78	0,78	5,13047	0,002674	0,0026734
			60	0,68	0,68	5,05478	0,00272	0,0026243
	550	0,013	0	0	0	1	0	0
			20	0,3	0,3	1,43302	0,000971	0,0009717
			30	0,3	0,3	1,45407	0,001029	0,0010199
			60	0,25	0,25	1,42637	0,001	0,0009564
		0,00875	0	0	0	1	0	0
			20	0,56	0,56	2,1982	0,001813	0,0018335
			30	0,5	0,5	2,12717	0,001714	0,001724
			60	0,45	0,45	2,14008	0,0018	0,0017439
		0,0045	0	0	0	1	0	0
			20	0,8	0,8	4,3045	0,00259	0,0026127
			30	0,75	0,75	4,25702	0,002571	0,002575
			60	0,64	0,64	4,13383	0,00256	0,0024774

Appendix D

Below is a list of detailed input value and results of the 70 examples solved for wrapped laminates and presented in Fig 29.

Nr	FRP	B/H	ρs	η	f'_c	f_y	ρ_s	h_f	t_{fv}	t_{fh}	$\overline{M_n}/M_n$	ρ_f(exact) exact	ρ_f(lin.reg) Linear reg.	difference (%)
1	G	0,5	0	1	50	550	0,013	60	0,5	0,5	1,1291	0,00219	0,0020016	8,425
2	G	0,5	0	1	50	550	0,0045	60	0,5	0,5	1,3885	0,00229	0,0022513	1,504
3	G	0,5	0	1	50	550	0,013	20	0,8	0,8	1,1635	0,00274	0,0025983	5,272
4	G	0,5	0	1	50	550	0,013	30	0,75	0,75	1,1643	0,00279	0,0026118	6,243
5	G	1	0	1	30	350	0,013	20	1	1	1,289	0,00314	0,0030391	3,301
6	G	0,8	0	1	30	350	0,013	20	1	1	1,289	0,00314	0,0030391	3,301
7	G	1	0,01	1	50	350	0,013	20	1	1	1,3024	0,00314	0,0031879	-1,433
8	G	1	0,002	1	30	350	0,013	20	1	1	1,2947	0,00314	0,0031025	1,286
9	G	1	0,002	1	50	550	0,013	20	1	1	1,1892	0,00314	0,0030446	3,125
10	G	1	0	1	30	350	0,013	30	1	1	1,2997	0,00329	0,0031575	3,902
11	G	0,8	0	1	30	350	0,013	30	1	1	1,2997	0,00329	0,0031575	3,902
12	G	1	0,002	1	30	350	0,0045	30	1	1	1,9049	0,00329	0,0034068	-3,687
13	G	1	0,002	1	50	550	0,013	30	1	1	1,1965	0,00329	0,0031711	3,488
14	G	0,5	0	1	50	550	0,0045	20	1	1	1,6116	0,00343	0,0035917	-4,759
15	G	1	0	1	30	350	0,013	60	1	1	1,3272	0,00371	0,0034611	6,816
16	G	1	0,002	1	50	550	0,013	60	1	1	1,2155	0,00371	0,0035009	5,744
17	G	1	0	1,5	30	350	0,013	30	0,8	1,2	1,3429	0,00377	0,0036348	3,624
18	G	1	0	2	50	350	0,013	20	0,63	1,259	1,3643	0,00378	0,0038716	-2,484
19	G	1	0	2	50	350	0,013	60	0,59	1,172	1,3643	0,00385	0,0038716	-0,548
20	G	1	0	1,5	30	350	0,013	20	0,88	1,314	1,3643	0,004	0,0038716	3,308
21	G	1	0	1,5	30	350	0,013	60	0,8	1,2	1,3643	0,00411	0,0038716	5,898
22	G	1	0	1,5	30	350	0,0045	20	1	1,5	2,2725	0,00457	0,0048122	-5,268
23	G	1	0	1,5	50	350	0,013	20	1	1,5	1,4394	0,00457	0,0047004	-2,822
24	G	1	0	1,5	30	350	0,0045	30	1	1,5	2,306	0,00471	0,0049404	-4,797
25	G	0,5	0	1,5	50	350	0,013	20	1	1,5	1,4649	0,00486	0,0049827	-2,586
26	G	0,5	0	1,5	50	350	0,0045	20	1	1,5	2,3646	0,00486	0,0051646	-6,331
27	G	1	0,002	1	30	350	0,013	30	1,5	1,5	1,4524	0,00493	0,004844	1,715
28	G	0,5	0	1,5	50	350	0,0045	30	1	1,5	2,4335	0,00514	0,005428	-5,545
29	G	1	0	1,5	50	350	0,013	60	1	1,5	1,451	0,00514	0,0048291	6,101
30	G	1	0,002	1	50	350	0,013	20	1,64	1,638	1,4935	0,00515	0,005298	-2,910
31	G	0,5	0	1	50	550	0,0045	30	1,5	1,5	1,9782	0,00557	0,0057939	-3,993
32	G	1	0,002	1	30	350	0,013	60	1,5	1,5	1,4935	0,00557	0,005298	4,907
33	G	0,5	0	1,5	50	350	0,013	60	1	1,5	1,5489	0,006	0,0059101	1,498
34	G	0,5	0	1,5	50	350	0,0045	60	1	1,5	2,6152	0,006	0,0061227	-2,046
35	G	1	0	2	50	350	0,013	20	1	2	1,5744	0,006	0,0061917	-3,195
36	G	1	0	2	50	350	0,0045	20	1	2	2,6866	0,006	0,0063956	-6,593
37	G	0,5	0	1	50	550	0,0045	60	1,33	1,331	2,0221	0,00608	0,006058	0,422
38	G	1	0	2	50	350	0,013	30	1	2	1,5859	0,00614	0,0063188	-2,863
39	G	1	0,01	1	50	350	0,0045	20	2	2	2,6662	0,00629	0,0063178	-0,510
40	G	0,5	0,01	2	30	350	0,013	20	1	2	1,6001	0,00629	0,0064758	-3,023
41	G	1	0,002	1	30	550	0,0045	20	2	2	2,0935	0,00629	0,006487	-3,202
42	G	1	0,002	1	50	350	0,0045	20	2	2	2,7344	0,00629	0,0065783	-4,654
43	G	1	0	1	30	350	0,0045	30	2	2	2,797	0,00657	0,0068177	-3,747
44	G	0,8	0	1	30	350	0,0045	30	2	2	2,797	0,00657	0,0068177	-3,747
45	G	1	0	2	50	350	0,013	60	1	2	1,616	0,00657	0,0066514	-1,217
46	G	0,5	0,01	2	30	350	0,013	30	1	2	1,623	0,00657	0,0067292	-2,401
47	G	1	0,002	1	30	550	0,0045	30	2	2	2,1348	0,00657	0,0067352	-2,492
48	G	1	0,002	1	50	350	0,013	30	2	2	1,6236	0,00657	0,0067351	-2,490
49	G	1	0	1,5	50	350	0,013	30	1,5	2,25	1,7157	0,00737	0,0077522	-5,166
50	G	1	0	1	30	350	0,0045	60	2	2	2,9672	0,00743	0,0074683	-0,535
51	G	0,8	0	1	30	350	0,0045	60	2	2	2,9672	0,00743	0,0074683	-0,535

52	G	1	0,002	1	30	350	0,0045	60	2	2	2,9576	0,00743	0,0074317	-0,043
53	G	1	0,002	1	50	350	0,013	60	2	2	1,6839	0,00743	0,0074009	0,373
54	G	0,5	0	1,5	50	350	0,013	30	1,5	2,25	1,7255	0,00771	0,0078611	-1,903
55	G	1	0	1,5	50	350	0,0045	20	2	3	3,5449	0,00914	0,0096774	-5,846
56	G	1	0	2	50	350	0,0045	30	1,5	3	3,5585	0,00921	0,0097291	-5,588
57	G	1	0,002	1	30	550	0,0045	60	2,5	2,5	2,5349	0,00929	0,0091391	1,579
58	G	1	0	1	30	350	0,0045	20	3	3	3,5484	0,00943	0,0096907	-2,780
59	G	0,8	0	1	30	350	0,0045	20	3	3	3,5484	0,00943	0,0096907	-2,780
60	G	1	0,002	1	30	350	0,0045	20	3	3	3,6388	0,00943	0,0100363	-6,446
61	G	1	0	1,5	50	350	0,0045	30	2	3	3,6118	0,00943	0,0099331	-5,351
62	G	1	0,01	1	50	350	0,013	30	3	3	1,932	0,00986	0,0101414	-2,884
63	G	1	0,01	1	50	350	0,0045	30	3	3	3,5849	0,00986	0,00983	0,276
64	G	1	0	2	50	350	0,0045	60	1,5	3	3,6905	0,00986	0,010234	-3,823
65	G	1	0,002	1	50	350	0,0045	30	3	3	3,6808	0,00986	0,0101969	-3,447
66	G	1	0	1,5	30	350	0,0045	60	2	3	3,7009	0,01029	0,0102737	0,117
67	G	0,5	0,01	2	30	350	0,013	60	1,5	3	2,0105	0,01114	0,0110091	1,200
68	G	1	0,01	1	50	350	0,0045	60	4	4	4,7617	0,01486	0,0145292	2,207
69	G	1	0,002	1	50	350	0,0045	60	4	4	4,8806	0,01486	0,0147841	0,492
70	G	1	0,01	1	50	350	0,013	60	4,5	4,5	2,5141	0,01671	0,0165711	0,857